Demonstrating the Priority of Lunar Orbital Port Over Lunar Surface Construction: A Descent Corridor with Electromagnetic Cargo Reception

Qin Chen

MicroIoT (Fuzhou) Network Technology Co., Ltd.

Building 7, Sansheng Binjiang International, Gangtou Plaza, No. 96 Nanjiangbin West Avenue, Cangshan District, Fuzhou, Fujian 350009, China

E-mail: fittelus@outlook.com

Abstract: This paper argues that the optimal place for humans to be stationed in lunar development is in lunar orbit rather than on the lunar surface. **Objective:** To test the mainstream premise that "lunar development must be based on the lunar surface"; to demonstrate the engineering rationale for building long-term habitation bases, production facilities, and logistics hubs in lunar orbit rather than on the surface; and to propose a system design for the "Lunar Orbital Port", a distributed system of circumlunar platform ports. **Methods:** On the basis of orbital mechanics (the vis-viva equation and the rocket equation), the velocity increments and mass penalties of lunar landing and departure were compared with those of residence in lunar orbit; the success rate of lunar soft-landing missions worldwide from 1966 to 2025 was tallied; scientific assessments were compiled on the Apollo moonquake network, the Chang'E-4 surface radiation measurements, and the health effects of lunar dust; and a model of ballistic delivery and electromagnetic regenerative deceleration capture was established for the "circumlunar platform – spindle-shaped ejection capsule – long-slope electromagnetic deceleration capture" architecture. **Results:** A one-way landing on the lunar surface requires a velocity increment of about 1.9 km/s (at I_{sp} = 300 s, propellant accounts for about 47.6% of the departure mass), and departure from the surface requires a further 1.85 km/s. The fully successful rate of lunar soft landings is about 50%, with failures concentrated in the powered-descent phase. The Apollo seismometers recorded shallow moonquakes of magnitude up to about 5, lasting from tens of minutes to several hours, far longer than the tens of seconds typical of terrestrial earthquakes. The radiation dose equivalent on the lunar surface is about 1.4 mSv/d (twice that on the International Space Station), and an extreme solar particle event of the 1972 type could deliver 3–4 Sv without shielding. Lunar dust is fine-grained, electrically charged, and angular; it is difficult to remove completely and causes irreversible damage to equipment and to the human respiratory system. With a frozen orbit, the annual station-keeping velocity increment in low lunar orbit can be held to 10–50 m/s, corresponding to a chemical propellant consumption of about 3–17 kg/t·a and an electric propulsion consumption of about 0.6–3.2 kg/t·a, comparable to or lower than the reboost level of the International Space Station (about 18 kg/t·a); ballistic delivery requires only about 23 m/s of ejection velocity increment and about 10 kg/t of propellant. For long-slope electromagnetic deceleration capture, a cargo of the 1 t class is loaded into a spindle-shaped payload capsule (total mass 1.2 t), which grazes into the original electromagnetic launch long slope at about 1.70 km/s and runs in the reverse direction; regenerative braking at the 30 g level requires about 5.4 km and lasts about 6 s, and about 79% of the kinetic energy (about 315 kWh per tonne of cargo) can be returned to storage, offsetting about 70% of the electricity consumed by an upward launch of the same mass. The contribution of kinetic-to-potential energy conversion on the slope is less than 0.04%, so the slope serves only for low-speed docking and controlled roll-back. Although orbits close to the Moon require more orbit control, they keep closer contact with the lunar surface and receive lower galactic radiation owing to shielding by the Moon itself; different orbits and distributed deployments should therefore be adopted according to actual requirements. **Conclusions:** Lunar-orbit platforms are superior to surface residence in energy, safety, environment, astronomical observation, and logistics efficiency in all respects. It is recommended that the primary construction layer of lunar development be placed in lunar orbit rather than on the surface, and that a "lunar orbit–lunar surface" materials corridor be opened by means of ballistic delivery at a controlled g-load (about 30 g), long-slope electromagnetic regenerative deceleration capture, and electromagnetic ejection (without

this corridor, construction of the Lunar Orbital Port would be pointless). If platforms and cargo adopt a momentum-exchange mode, large amounts of propellant and energy can be saved, and efficient descent of cargo can be coupled with platform orbit changes and orbit maintenance. The paper also proposes storing the residual hulls of spacecraft in lunar orbit as a reserve of scarce metals.

Keywords: Lunar orbit; Lunar Orbital Port; lunar base; soft landing; mascons; frozen orbit; lunar dust; radiation protection; in-orbit manufacturing; lunar development; reuse of discarded hulls; ballistic delivery; electromagnetic deceleration; long-slope capture; regenerative braking; energy recovery

---

1 Introduction

Since the Apollo era, human designs for lunar development have rested on one key premise: almost all engineering and infrastructure for residence on the Moon is built on the lunar land surface. The global space community (including NASA's Artemis and CNSA's ILRS) envisions lunar development mainly as the construction of permanent bases on the lunar surface, treating surface missions as the principal operating layer and rarely addressing lunar space. Both of the current international cooperation frameworks, namely the US-led Artemis Accords [38] and the memorandum of understanding for the International Lunar Research Station (ILRS) led by China and Russia [39], as well as the Commercial Lunar Payload Services (CLPS) program, take "landing–construction–residence" as the standard path for their early testing, development, and verification. However, of the 48 lunar soft-landing attempts from 1966 to 2025, only 24 were fully successful, a success rate of about 50% [10–12, 14, 15], and the failures were overwhelmingly concentrated in the powered-descent and landing-control phases; even among the successes, "landings with injuries" such as tipping over or attitude anomalies recurred [13, 15], greatly reducing mission completion. Taken together, these facts suggest that making lunar-surface landing the precondition of large-scale development is costly and fragile in engineering terms, and whether this collective path lock-in can withstand engineering-economic scrutiny has not yet been systematically questioned.

A variety of engineering experience shows that the lunar surface environment is extremely harsh, for example:

1. **A high gravity-well penalty:** Moving material from lunar orbit to the lunar surface and back to lunar orbit requires a one-way ΔV expenditure of at least 1.68–2.38 km/s; once gravity losses and guidance and control margins are taken into account, **the actual powered-landing requirement can be higher than this value,** which severely compresses the payload fraction.
2. **Lunar dust (regolith/lunar dust) poses extremely high engineering risk:** Lunar dust is electrostatically charged and sharp-edged, and it causes irreversible damage to mechanical drives, seals, optical lenses, and the human respiratory system.
3. **Dynamic environmental threats:** Shallow moonquakes are long in duration (up to several hours) and have a strong cumulative energy effect; the lunar surface lacks atmospheric protection, and direct exposure to micrometeoroids and to solar and galactic cosmic radiation (SPE/GCR) is a great threat.

In contrast, the operation and maintenance of spacecraft in planetary orbit has decades of mature experience, and the technology readiness level (TRL) of orbital rendezvous for crew handover and cargo transfer in space has reached 8–9 (for example Apollo, the ISS, and Tiangong), with safety and reliability that are orders of magnitude higher than those of a landing on the lunar surface. This has already been

verified: platforms such as the Lunar Reconnaissance Orbiter (LRO) and the Chandrayaan-2 orbiter have operated stably in low lunar orbit for long periods, and the orbit-maintenance requirement is far lower than intuition would suggest (for example, at an altitude of 50 km LRO needs only one orbit-maintenance maneuver every 28 days to keep its orbit within the permissible range of 35–65 km and avoid impact with the lunar surface, and it has operated stably for more than 17 years). The core arguments of this paper are: (1) shifting the center of gravity of lunar development from the lunar surface to far-lunar or near-lunar orbits is not only more feasible technically but also more reasonable economically; and (2) in scenarios such as one-way delivery of materials, in-orbit manufacturing, and orbital observation, moving the front-loaded center of lunar development to near-lunar orbit is technically feasible and has potential economic advantages (see Section 3.7 for the break-even analysis). The strategic logic of this shift can be summarized as "sky first, ground later": first establish a sustainable presence in lunar space, and then extend progressively from lunar space to the lunar surface. This view is also based on a thought-provoking question: even verification of near-Earth round trips took many years of repeated, expensive, and arduous practice, so how much more so for an unfamiliar planet 380,000 km away? The paper also reveals that the orbital environment in space is far more favorable than the lunar surface in terms of the conditionality and the controllability of construction (relay bases suitably located in orbit can serve as assembly nodes for Earth–Moon transportation and lunar surface missions; whether LLO, DRO, NRHO, or another orbit is adopted should be determined by trading off multiple objectives such as transportation, maintenance, illumination, and communications).

This paper presents the theoretical framework of "Orbit-First, Sky-Ground Coupling". Preferably, large modular "circumlunar platform ports" (also called the distributed "Lunar Orbital Port") are established in low lunar orbit (altitude 30–200 km) as the hub for human production, living, scientific research, and computing, and high-frequency one-way delivery of materials to the lunar surface is achieved by means of "long-slope electromagnetic regenerative deceleration" technology, thereby avoiding large-scale, high-cost infrastructure construction on the lunar surface in the early stage. The reasons for this contrary proposition can be summarized in five points. First, landing on the lunar surface consumes energy for deceleration and departing from it consumes energy for acceleration, so the energy cost per unit mass is far higher than that of orbital residence; landing is technically difficult and has a high failure rate (it should be noted, however, that ballistic delivery does not eliminate kinetic-energy dissipation but transfers it to the deceleration and energy-recovery task of the long-slope electromagnetic installation on the lunar surface; see Sections 4.2.2 and 4.2.3). Second, a lunar surface base must at all times withstand moonquakes and meteoroid strikes, whereas spacecraft in orbit operate smoothly and can be warned of hazards and maneuver to avoid them. Third, astronomical observation from the lunar surface is limited in viewing geometry, whereas reconfigurable interferometric arrays of clusters in lunar orbit can perform wide-field sky surveys and form ultra-long baselines with Earth, the lunar surface, and deep-space platforms. Fourth, the lunar surface is afflicted by both cosmic radiation and lunar dust, whereas metallic orbital modules with multiple protective liners can shield most of the radiation and are free from the harm of lunar dust. Fifth, a relay base in a far-lunar orbit is a natural "good harbor in the sky" for the movement of people and the transfer of materials. The paper also explains that high-orbit options such as the near-rectilinear halo orbit (NRHO) have advantages in insertion velocity increment and communication continuity [48], but their perilune altitude reaches several thousand kilometers, which cannot support the low-orbit ballistic delivery described in this paper; the far and near options therefore suit different scenarios (see Section 3.6).

On the basis of the above arguments, this paper further presents a design for the "Lunar Orbital Port" system: a low-lunar-orbit platform port serves as the relay and delivery hub; the "circumlunar platform – spindle-shaped ejection capsule – long-slope electromagnetic deceleration capture" architecture achieves low-cost soft-landing delivery to the lunar surface (borrowing and reversing the original electromagnetic launch long slope, with regenerative braking along the track and energy recovery); electromagnetic delivery achieves upward transport of materials from the lunar surface; and storage of residual vessel hulls in lunar orbit achieves a materials cycle between Earth and the Moon. All numerical calculations in the paper are given with their methods and assumptions (see Appendices A and B), and all external facts are accompanied by references. This paper strives to turn "orbit first" from a concept into a calculable engineering system, and to provide preliminary quantitative models for delivery, energy management, and the materials cycle. The paper is positioned as a concept study: all conclusions are conditional on the assumptions made in the text, and the limitations are discussed mainly in Section 4; the break-even analysis (Section 3.7) and the delivery guidance and deceleration analysis (Section 4.2.2) are the keys to evaluating the feasibility of this system.

2 Engineering Costs of the Lunar-Surface Residence Paradigm

2.1 Energy Costs of Landing on and Departing from the Moon

Although the Moon's gravity well is far shallower than that of Earth (escape velocity 2.38 km/s versus 11.2 km/s), the characteristic velocity required for "landing and departure" is still considerable. Taking the Apollo missions as the baseline: lunar orbit insertion (LOI) required about 0.91 km/s [44]; the descent of the lunar module from a lunar orbit of about 110 km to the surface, including hover and terminal maneuvers, required about 1.7–2.0 km/s over the whole course [43, 45]; and the ascent stage returning from the lunar surface to lunar orbit required about 1.85 km/s (the Apollo 11 measured value was 6,055 ft/s ≈ 1,846 m/s) [43]. Consequently, a lunar-segment round trip "to the lunar surface and back" requires an additional ΔV of about 3.7–3.9 km/s, and this does not yet include the structural mass of the lander itself (such as the mass of the lander structure, thermal control, navigation, landing legs, and redundant systems). According to the rocket equation $\Delta V = I_{sp} \cdot g_0 \cdot \ln(m_0/m_1)$, taking a specific impulse I_{sp} = 300 s (g_0 = 9.81 m/s²): the propellant required for a one-way landing ($\Delta V \approx 1.9$ km/s) is about 47.6% of the departure mass, and for a landing–ascent round trip ($\Delta V \approx 3.7$ km/s) it is as high as 71.6%. The Apollo lunar module had a total mass of 14,696 kg, of which 10,523 kg was propellant, so the propellant fraction was exactly 71.6% [45]. The historical data and the theoretical calculation agree in order of magnitude (the actual I_{sp} and ΔV allocation of the lunar module are not exactly the same as the values used in this paper, so this agreement should be regarded as an order-of-magnitude check). This means that for every 1 t of payload soft-landed on the lunar surface, a lander of about 2.9 t must first be assembled in lunar orbit (LLO) (payload 1.0 t + structure 0.5 t + propellant 1.36 t). If round trips of crew are taken into account, the energy cost of the surface paradigm is multiplied further.

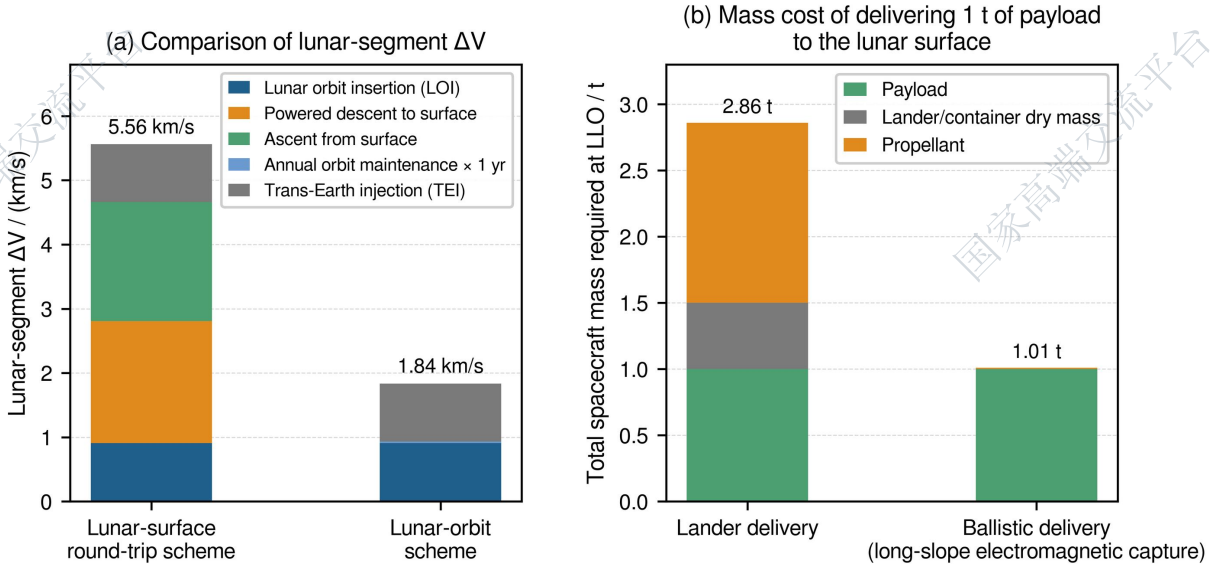


Fig. 1. Comparison of the lunar-segment velocity increments of lunar-surface residence and lunar-orbit residence (a), and of the mass cost of delivering 1 t of payload to the lunar surface (b)

According to the Tsiolkovsky equation:

$$\Delta V = I_{\mathrm{sp}} g_0 \ln(m_0/m_1) \tag{1}$$

Assume a descent from low lunar orbit (h = 100 km, orbital speed v of about 1.63 km/s) to the lunar surface with a complete landing. The theoretical minimum ΔV required is about 1.68 km/s; allowing for gravity losses, attitude control, and deceleration margins, the actual engineering consumption is about 2.1–2.4 km/s. Taking off from the lunar surface to return to low lunar orbit requires a further ΔV of about 1.8–1.9 km/s. (The above 1.68 km/s is the ideal lower limit that excludes gravity losses; the Apollo measured descent phase, including hover and maneuvers, was about 1.7–2.0 km/s. Throughout this paper the one-way landing interval is expressed uniformly as 1.7–2.4 km/s, and the calculation examples take 1.9 km/s.)

By comparison, maintaining a circular or frozen orbit (frozen orbit, for example at inclinations i = 27°, 50°, 76°, 86°) at an altitude of 100 km is subject mainly to perturbations from the non-spherical gravitational potential bias caused by the lunar mass concentrations (mascons) (higher-order harmonics such as J_2, C_{22}, and C_{20}). The energy required for a spacecraft to maintain stable operation in lunar orbit is therefore very small (see Section 3.1): mascon perturbations and three-body effects are the main perturbation sources in low lunar orbit [1–4], and since the Moon has no atmosphere there is no atmospheric drag term and no fluctuation with the solar activity cycle.

Appendix: Calculation of station-keeping consumption for different propellants: (The values below are taken for a frozen orbit with an annual maintenance ΔV of 10–50 m/s and converted by the rocket equation; very low orbits and polar orbits are higher, see Section 3.1.)

For a spacecraft in an uncorrected low lunar orbit, mascons cause the orbital eccentricity to drift, so that the perilune gradually descends until the spacecraft impacts the lunar surface. Through active control with electric propulsion (Hall effect thruster, I_{sp} of about 1500–3000 s) or micro cold-gas thrusters, however, the calculation gives:

- **Cold-gas thrusters (I_{sp} = 73 s):** annual average propellant consumption of about 14–69 kg/t;

- **Chemical propulsion (I_{sp} = 300 s):** annual average propellant consumption of about 3.3–16.3 kg/t;
- **Hall electric propulsion (I_{sp} = 1600 s):** annual average propellant consumption of only about 0.6–3.2 kg/t;
- If an inter-platform cargo kinetic-energy exchange system is implemented, dependence on propellant can be partly eliminated when two-way logistics are balanced (discussed quantitatively in Section 3.3).

More specific orbit-maintenance costs are given in Section 3.1. In short, the cost of "going up there once" and that of "parking there" differ by about two orders of magnitude; this is the energetic basis of all the arguments in this paper, and it is therefore of great significance for the related "long-term, large-scale, continuous ballistic delivery of materials" (see Section 3.7).

2.2 Technical Risks of the Landing Phase: Historical Statistics

Table 1 summarizes the lunar soft-landing attempts worldwide from 1966 to 2025. The Soviet Luna series suffered 11 consecutive soft-landing failures from 1963 before Luna 9 succeeded on its twelfth attempt; the US Surveyor program succeeded 5 times out of 7; all 6 crewed Apollo landings succeeded, although Apollo 13 was abandoned before landing because of a service-module failure; and in the 21st century, Chandrayaan-2 "Vikram" (2019), Beresheet (2019), Hakuto-R M1 (2023), Luna 25 (2023), Peregrine (2024, which did not reach the lunar surface), IM-2 "Athena" (2025), and Hakuto-R M2 (2025) all failed, with the causes concentrated in the engine, ranging, and guidance elements of the powered-descent phase [11, 12, 14, 15]. IM-1 "Odysseus" and SLIM soft-landed successfully but tipped over by about 30° and touched down nose-down, respectively; these immobilized spacecraft achieved only some of their mission objectives [13, 15]. In total there were 48 attempts, 24 full successes, 3 partial successes, and 21 failures, a full-success rate of about 50% (Fig. 2).

Table 1. Statistics of lunar soft-landing missions (1966–2025)

Decade	Principal missions	Attempts	Full successes	Partial successes	Failures (main cause/phase)
1960s	Soviet Luna 9/13, etc. (13 missions); US Surveyor (7 missions)	20	7	0	13 (mainly powered descent/crash into the Moon)
1970s	Luna 15–24 (8 missions); Apollo 11–17 (6 missions)	14	11	1	2 (Luna 15/18 crashed; Luna 23 tipped over)
2010s	Chang'E-3/4, Vikram, Beresheet	4	2	0	2 (loss of control in descent phase)
2020–2025	Chang'E-5/6, Chandrayaan-3, SLIM, Hakuto-R ×2, Luna 25, IM-1/2, Blue Ghost 1	10	4	2	4 (ranging/engine/guidance)
Total	—	**48**	**24**	**3**	**21**

Note: Because Peregrine did not reach the lunar surface, it is not counted as a "landing attempt"; partial success means that a soft landing was achieved but attitude or operating capability was impaired. Data sources [10–15].

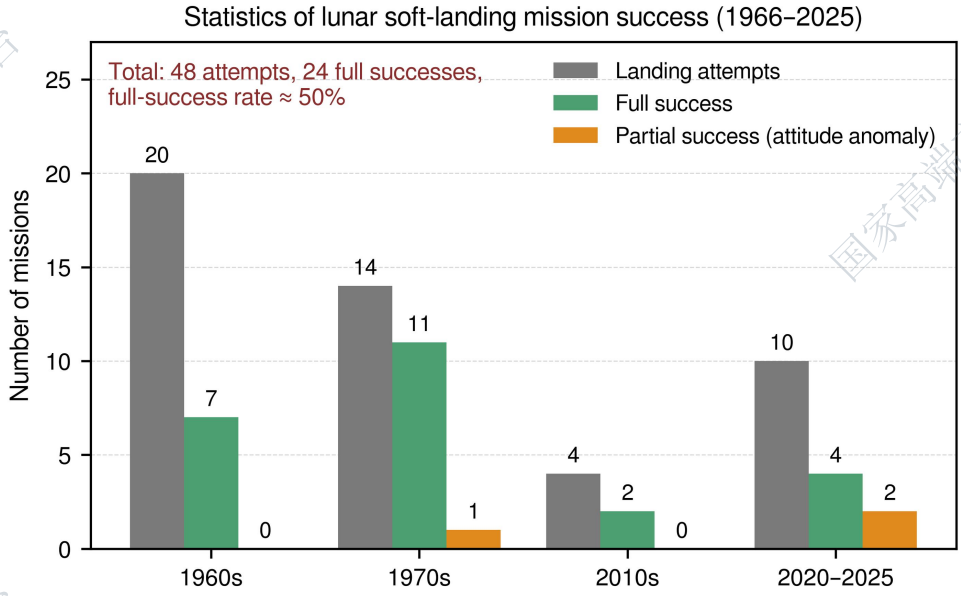


Fig. 2. Statistics of lunar soft-landing mission success (1966–2025). Data sources [10–15]

The above statistics reveal a fact obscured by the "moon-landing success narrative": soft landing is not a mature technique but a long, struggling curve of failure and success, and it is not yet a mature technique that can be replicated in large quantities at low cost; its reliability improves as operating entities accumulate experience, but remains uneven. The difficulty lies in the fact that the Moon has no atmosphere and aerodynamic deceleration is impossible: the entire velocity increment must be expended by retro-engines within the last dozen or so minutes, relying throughout on precise closed-loop powered deceleration (Powered Descent Initiation, PDI); failure of any one of terrain sensing, lidar hazard avoidance, ranging, hovering, or landing-leg cushioning can be fatal, which places extremely high demands on real-time feedback and control. If the lunar surface were developed on a large scale, with daily landing frequencies in the hundreds, then at the current success rate failure would be the norm rather than the exception. Classic failure modes reveal a structural dilemma: every link of a lunar surface landing (communications, sensing, guidance, and propulsion) must cooperate precisely under "one-shot, irreversible" conditions, and an anomaly in any single link can lead to the failure of the entire mission. The conclusion of Doan, an engineer at NASA's Marshall Space Flight Center, is worth quoting verbatim: "Landing is a high-risk phase of lunar missions, mainly because plume interaction interferes with telemetry and communications. Loss of communication should be regarded as an expected event, which increases reliance on sensor readings during landing."

A common rebuttal is that, with technological progress, the reliability of lunar surface landing will eventually improve, and that the current failure rate does not represent future levels. This argument certainly holds in the long run, since technology does advance, but time does not wait: while waiting through the long period for the technology to mature, a better scheme already exists that avoids the above complex process altogether and turns fragmentary landings into a permanent delivery-and-reception infrastructure, so why not implement it as early as possible? A lunar-orbit platform, close to the Moon, undoubtedly offers the convenience of carrying out technical verification at any time, which will help to shorten greatly the cycle for perfecting the above technologies and thereby achieve safer, crew-rated lunar landing. Even if the landing success rate were raised to 100%, the energy penalty from low lunar orbit to the lunar surface would remain, and every kilogram of cargo would still have to pay a "landing tax" of about 1.7 km/s, in addition to the many related supporting needs that must be

established, such as spacecraft operation and maintenance, wear and depreciation, and logistics scheduling.

Ballistic delivery from lunar orbit, by contrast, reduces the velocity increment of "delivering goods to the lunar surface" to about 23 m/s, and the transferred energy is largely converted into a change of spacecraft momentum and into electric energy recovered by the long-slope electromagnetic installation (Section 4.2.3); its evident advantage is that it fundamentally **bypasses** the energy penalty rather than optimizing the penalty internally. Ballistic delivery reduces the velocity increment on the platform side to about 23 m/s and removes the need to carry landing propellant with the cargo; but it must be made clear that the cargo still carries about 1.45 GJ/t (about 401 kWh/t) of kinetic energy on reaching the Moon. This energy has not vanished but is borne instead by energy-dissipating/absorbing facilities fixed on the lunar surface (about 79% of which can be recovered as electric energy by long-slope regenerative braking; see Section 4.2.3). The essence of ballistic delivery is therefore to replace propellant mass that is "carried with the cargo and consumed every time" with permanent lunar-surface infrastructure that is "built once and used repeatedly"; whether it is superior depends on the total delivered mass (the break-even analysis in Section 3.7) and on the mass and reliability of the long-slope deceleration facility (Section 4.2.3).

2.3 Hazards of the Lunar Surface Environment

2.3.1 Moonquakes

The Apollo seismic network (1969–1977) records show that the Moon is not a seismologically "dead" body [16–18]: only 28 shallow moonquakes were recorded in 8 years, but 7 of them had body-wave magnitudes above 5, the largest event had an energy exceeding 6×10^{10} J, and the focal depths were about 50–200 km; deep moonquakes number from several hundred to over a thousand per year, mostly concentrated at depths of 700–1,200 km with body-wave magnitudes below 2–3; and there are also thousands of thermal moonquakes (caused by thermal expansion and contraction of the lunar surface). The lunar crustal medium attenuates seismic waves very weakly, so the shaking from one moonquake can last from tens of minutes to several hours, far longer than the tens of seconds of terrestrial earthquakes. For lunar surface buildings and equipment, prolonged excessive swaying under low gravity easily becomes a nearly saturated fatigue load. The local intensity of shallow moonquakes is sufficient to cause serious damage to precision equipment and structures, which places demands far harsher than terrestrial standards on structural design and materials research; spacecraft in lunar orbit, by contrast, are completely decoupled from the lunar crust and wholly unaffected by moonquakes. Analysis: the 28 shallow moonquakes were distributed over the whole Moon and spanned 8 years, an average of about 3.5 per year; for any particular site, the probability of a strong moonquake is far lower than in the seismically active regions of Earth. The hazard of moonquakes to lunar surface bases will manifest mainly as seismic design loads and long-term fatigue rather than as a frequent disaster, and should be managed through site selection, foundation isolation, and seismic monitoring; although it is not regarded as an insurmountable obstacle, in terms of the seismic standards of the facilities it is a cost that every construction must bear.

2.3.2 Meteoroid Impacts

The Moon has no atmosphere, so meteoroids can strike the lunar surface without attenuation. It is estimated that the Moon receives about 1.4 t of meteoroid material per day [20]; a lunar surface base would be struck each year by about 1.5×10^{4}–2.3×10^{4} micrometeoroids with masses of 10^{-6}–10 g [21],

and meteoroids larger than a table-tennis ball occur about 3.3×10^4 times per year; LRO observations show that the Moon gains a new impact crater about 50 m in diameter every year [21]. The cumulative effect of tiny impacts not recorded by instruments is difficult to estimate quantitatively and should be considered as a design margin. On April 7, 2026, during the Artemis II circumlunar mission, when the Orion spacecraft was about 46,000 miles from the Moon, the crew reported seeing five faint "pinprick"-like flashes within a short time, all of which were caused by rock fragments striking the lunar surface.



Fig. 3. Hand-drawn map by the astronauts of the locations of lunar-surface "flashes"; lunar meteoroid impacts are regarded as high-frequency events. (Blue marks by Reid Wiseman; green marks by Victor Glover; red marks by Jeremy Hansen)

For critical facilities with long-term duty (for example, nuclear power stations), cumulative exposure is inevitable. Permanent lunar surface facilities must therefore be covered with high-strength structures and protective layers, which greatly increases construction cost, whereas an orbital platform can rely on ground- and space-based monitoring networks for early warning and, when necessary, perform evasive maneuvers with a small amount of propellant, turning meteoroid risk from something to be "endured" into something to be "managed". Going a step further, valuable facilities could even be protected (by self-sacrificial active intervention against certain meteoroids that must be intercepted), and would become a protective barrier for both the Moon and Earth (for potential celestial threats, the earlier the intervention, the more pronounced the effect).

2.3.3 Radiation

Measurements by the Lander Neutron and Dosimetry (LND) payload on the Chang'E-4 lander give an absorbed dose rate on the lunar surface of about 13.2 μGy/h (in silicon), of which neutral particles (neutrons and gamma rays) account for about 23%, and a dose-equivalent rate of about 60 μSv/h, that is, about 1.4 mSv/d, about twice the contemporaneous level on the International Space Station (about 0.7 mSv/d) [22]. The galactic cosmic ray (GCR) background fluctuates between about 0.5 and 1.4 mSv/d with the solar activity cycle; more dangerous are solar particle events (SPEs). For the extreme SPE of August 1972, which occurred between Apollo 16 and Apollo 17, the estimated dose to astronauts exposed on the lunar surface in spacesuits at that time would have been of the order of 3–4 Sv (higher at the body surface) [23]. It can be seen that the radiation environment facing lunar surface residents is exceptionally harsh, and the cancer risk from long-term exposure rises markedly. By contrast, equivalent

aluminum shielding of about 20 g/cm² on a spacecraft can reduce the dose from such an event by about 94% (from about 4,000 mSv to about 230 mSv) [23]; lunar-orbit platforms should use metallic cabin walls supplemented with water/polyethylene liners for radiation shielding, taking advantage of the shielding provided by the naturally present half-sphere and of the areas where one can take shelter during an SPE. The blocking fraction varies with orbital altitude; for example, calculated with the Moon's mean radius of 1737.4 km, the geometric blocking by the Moon of the 4π solid angle is about 34% in a 100 km orbit, about 41% at 30 km, and about 28% at 200 km. The arrival direction of SPE particles varies with time and the platform moves continuously around the Moon, so blocking by the Moon can provide partial shielding over some orbital arcs. With personnel working inside a storm shelter equipped with complete protective measures, the combined protection can approach that of lunar lava tubes, which, although widely expected to be habitable, have not yet had their actual number and volume established.

Table 2. Comparison of radiation-environment doses

Scenario	Dose-equivalent rate / (mSv/d)	Remarks
Earth surface (background)	≈ 0.0066	Natural background (including radon, etc.)
ISS (LEO ≈ 400 km)	≈ 0.7	Measured in low Earth orbit [22]
Deep-space transfer (cruise)	≈ 1.8	Measured by MSL RAD during the cruise phase [49]
Lunar surface (Chang'E-4 LND)	≈ 1.4	Absorbed dose 13.2 μGy/h; dose equivalent ≈ 60 μSv/h [22]
Lunar-orbit cabin (20 g/cm² equivalent shielding)	1.1–1.3 (estimated)	Estimated from MSL RAD measurements after deducting 28%–41% blocking by the Moon (Appendix B)
1972-type SPE (single event)	3–4 Sv unshielded; ≈ 0.23 Sv with 20 g/cm² shielding	NASA 1988 estimate and shielding modeling [23]

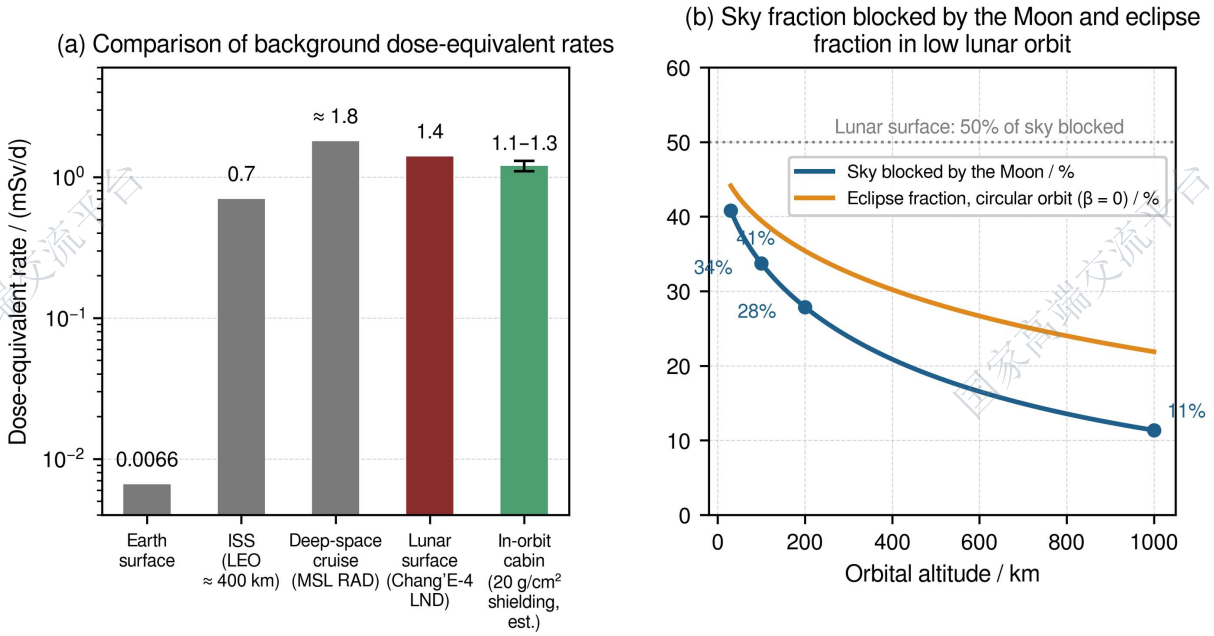


Fig. 4. (a) Comparison of background dose-equivalent rates; (b) fraction of the sky blocked by the Moon and fraction of the orbit spent in lunar eclipse in low lunar orbit (calculated in this paper; formulas in Appendix B)

2.3.4 Lunar Dust

The threat of lunar dust is far more than the word "inconvenience" can convey. Studies cited in NASA's lunar dust technical brief show that the output power of photovoltaic cells falls by 50% when the dust

coverage is only 3 mg/cm². Lunar dust is angular and sharp and readily penetrates seals, connectors, bearings, optical lenses, and spacesuit joints, leading to performance degradation and a sharp rise in maintenance needs. The failures of several commercial missions show that lunar dust raised by the plume of the landing engine can obscure laser rangefinders and optical sensors and also interfere with radio communications. Post-mission investigations confirmed a direct correlation among sensor contamination, solar panels covered by lunar dust, damage to communication antennas, and lander tipping.

More serious are the health risks: NASA's human system risk analysis indicates that lunar dust exposure is associated with eye injury, lung injury, and skin irritation, and that the potential consequences of long-term exposure include pneumoconiosis, hypersensitivity, and even cancer. The charged nature and submicron particle size of lunar dust make it difficult to remove completely by conventional filtration, and frequent filter replacement itself adds to the consumption of supplies and to crew time.

Lunar regolith and dust are the most "ineradicable" threat to lunar surface residence [24–26]: fine particles (< 10 μm, respirable) make up a considerable proportion and, once charged, levitate electrostatically and adhere to every surface; inside the Apollo astronauts' return cabins, "lunar hay fever", eye and nose irritation, and respiratory symptoms appeared, and the filters could not remove the fine dust, so that allergic reactions worsened after repeated exposure [24, 25]. Lunar dust poses continuous harm to seals, bearings, optical devices, and the human respiratory tract. Lunar-orbit platforms are entirely in a dust-free environment, so the lunar dust problem disappears at its source, and only the docking and extravehicular-exit steps need to be managed through airlocks and blow-off procedures.

Table 3. Comparison of lunar surface environmental hazards and lunar-orbit residence

Hazard dimension	Lunar-surface residence	Lunar-orbit residence
Moonquakes	Shallow moonquakes up to about magnitude 5, with shaking lasting tens of minutes to several hours, imposing fatigue loads on structures [16–18]	Decoupled from the lunar crust; unaffected
Micrometeoroids/meteorites	1.5×10^4–2.3×10^4 impacts per year; heavy protection required [20, 21]	Evasive maneuvers possible after warning; protection mainly by granular skirt panels
Radiation	Background ≈ 1.4 mSv/d; SPEs can reach the Sv level with nowhere to hide [22, 23]	Metallic cabin walls + water/polyethylene shielding; the Moon blocks only about 28%–41% of the sky; combined with a storm shelter [23], a background of the same order as on the lunar surface is achieved
Regolith/lunar dust	Ubiquitous and ineradicable; harms respiration and equipment [24–26]	Dust-free environment; only docking/extravehicular-exit management required
Temperature cycling	Extreme thermal cycling of the order of 300 K over the day–night cycle; frequent thermal moonquakes	Stable illumination in orbit; simplified thermal-control design
Observation field of view	Lunar horizon limited; dust deposition contaminates optical surfaces	Whole-sky surveying, with no dust or thermal cycling; radio silence possible during far-side arcs [40, 41]
Logistics	Landing and departure require 3.7–3.9 km/s; high failure rate	Link-up with ballistic/electromagnetic delivery; platform-side propellant consumption markedly reduced; total cost depends on the delivered mass (Section 3.7)

2.3.5 Psychophysiological Factors

The monotony of the lunar surface environment, the isolation of confined spaces, ever-present lunar dust, the meteoroid threat, and even the survival pressure of being "unable to leave at any time" all pose long-term challenges to the psychological and physiological health of crews. A lunar-orbit platform, by contrast, faces space and sees the home planet more often; distributed Moon-patrolling platforms offer construction that can be visited and inhabited at any time, and their markedly different styles can relieve mind and body, while artificial gravity simulates the Earth experience. At the very least, crews in orbit retain the possibility of rapid evacuation back to Earth by maneuvering.

2.4 Resource and Logistics Bottlenecks of Lunar Surface Construction

In-situ resource utilization (ISRU) on the lunar surface, although highly anticipated, requires complete sets of equipment for oxygen production, smelting, building materials, and so on to be brought from Earth and operated for long periods at high energy consumption, so that it is difficult to become self-sustaining in the short term [26]. Although the presence of water ice in the lunar polar regions has been confirmed [28, 29], it is concentrated in permanently shadowed regions (PSRs), whose low temperature, low illumination, and complex terrain make mining and residence extremely difficult; the so-called permanently sunlit regions are small in area, and competition for sites within the limited space is likely to cause disputes. The construction cycle of a lunar surface base is long, movement of personnel is inconvenient, residents are trapped on the surface, and living facilities are rudimentary. All of these constitute systemic bottlenecks of the lunar surface paradigm.

A lunar orbit, by contrast, spends long periods in space with ample sunlight, and the night-side interval through which it passes quickly is brief (the eclipse time of a near-circular orbit is 22%–44% of the period, corresponding to altitudes of 1,000–30 km; a 100 km orbit has about 39%, about 46 min per revolution, with about 4,500 storage-battery cycles per year, and is not a total eclipse; choosing an orbit with a high solar β angle, close to the terminator, can shorten or even eliminate the eclipse markedly). Compared with the lunar surface, on which day and night divide a 28-day cycle equally, the Moon-patrolling cycle ensures a stable energy supply. As for the drawback of microgravity on orbital platforms, rotating artificial-gravity sections can be installed in some segments to house a small number of personnel, with water, air, and thermal circulation systems and with cultivation of plants, approximating the Earth environment as far as possible. (Note: the 1/6 g on the lunar surface is likewise far below 1 g; a lunar-orbit platform can provide artificial gravity through rotating sections with a clear upgrade path, whereas adding artificial-gravity facilities on the lunar surface is almost infeasible.)

3 Engineering Advantages of Lunar Orbit

3.1 Orbit-Maintenance Cost: Mascons, Frozen Orbits, and Propellant Accounting

Lunar orbit is not entirely "free": the lunar surface mascons (mass concentrations) discovered in 1968 cause marked perturbations in low orbit and can make an uncontrolled circular orbit at the 100 km level decay into impact with the lunar surface within a few months [1, 2]; the GRAIL mission advanced the spherical-harmonic model of the lunar gravity field to degree 900 (GRGM900C), so the perturbation sources can now be modeled and predicted accurately [3]. NASA's analysis of LRO showed that a 50 km circular polar orbit is not naturally stable and, without control, could lead to impact with the Moon within about 41 days owing to the Moon's non-spherical gravity; LRO was therefore allotted a

station-keeping Δv budget of 150 m/s per year. It should be explained that 150 m/s·a corresponds to an under-stable 50 km circular polar orbit; the 10–50 m/s·a in Table 4 applies only to inclinations that can be frozen (near about 27°, 50°, 76°, and 86°) and to altitudes of 100–200 km. When a polar orbit is chosen in order to reach the polar regions, the maintenance cost lies between the two and must be calculated orbit by orbit. Combining the existing studies, a 30 km-class very low polar orbit, a 100–200 km frozen orbit, and a high orbit of about 1,000 km can be taken as candidate intervals of different maintenance-cost levels; for example, among the mature countermeasures already available, the frozen orbit can suppress the long-term perturbation terms: after LRO entered orbit in 2009, it was transferred in December 2011 into a quasi-frozen elliptical near-polar orbit (about 30 km × 180 km) whose perilune is controlled and stable, and forecasts show that it can be maintained beyond 2030 without large maneuvers [5]; a Korean study of very-low-orbit maintenance gives an annual maintenance ΔV of about 35–65 m/s for orbits of the 15–30 km class under ±5 km/±10 km dead bands [6]; and recent research even proposes zero-propellant maintenance of very low lunar orbits by means of solar sails [7]. Taken together, the typical orders of magnitude of the annual orbit-maintenance ΔV for lunar orbits are: 35–65 m/s for a 30 km-class very low polar orbit, 10–50 m/s for a 100–200 km frozen orbit, and 1–10 m/s for a high orbit of about 1,000 km [6–8]. China's lunar relay communication satellite also adopts a frozen-orbit design to reduce maintenance cost markedly [37]. All of this shows that it is feasible to reduce maintenance cost by using particular families of dynamical orbits.

Table 4. Lunar-orbit parameters and annual maintenance cost (per unit mass; parameters in Appendix B)

Orbit	Period / h	Circular speed / (km/s)	Annual maintenance ΔV / (m/s, estimated)	Chemical propellant / (kg/t·a)	Electric-propulsion propellant / (kg/t·a)
LLO 30 km	1.85	1.666	35–65	12–22	2.2–4.2
LLO 100 km (frozen)	1.97	1.633	10–50 (typical 25)	3.4–16.8 (typical 8.5)	0.6–3.2 (typical 1.6)
LLO 200 km (frozen)	2.13	1.591	5–30 (typical 15)	1.7–10.2 (typical 5.1)	0.3–1.9 (typical 1.0)
High lunar orbit ~1,000 km	3.57	1.338	1–10 (typical 3)	0.3–3.4 (typical 1.0)	0.06–0.6 (typical 0.2)
Reference: ISS (LEO ≈ 400 km)	1.55	7.67	≈ 57	≈ 17.9	—
Reference: GEO	23.93	3.07	40–50	≈ 13.6–16.9	—

Note: Propellant masses are first-order conversions of the ΔV intervals in the table by the rocket equation, with I_{sp} = 300 s (chemical) and I_{sp} = 1,600 s (electric propulsion); the ISS annual reboost $\Delta V \approx 57$ m/s and propellant of about 7.5 t/a (total mass about 420 t) are given only as an order-of-magnitude comparison and are not intended to prove cost equivalence between the two kinds of space infrastructure [8].

Table 4 and Fig. 5 show that for medium and low lunar orbits operated as frozen orbits, the annual maintenance cost is comparable to or lower than the reboost level of the International Space Station; if electric propulsion (Hall or ion) is adopted, propellant consumption can be reduced to the order of about 1 kg per tonne per year (1‰). An unloaded electrically propelled platform can maintain its orbit almost "permanently" with solar energy replenishment; if cargo ejection (see Section 4.3) is used as the source of propellant, orbit maintenance and delivery of materials merge into one, spreading the cost further. In theory, the momentum change produced by the ejection of part of the cargo can be incorporated into platform orbit control, thereby reducing additional propellant requirements; but the ejection mechanism, cargo losses, and energy cost must be included in the system budget. For comparison, satellites in low Earth orbit must continually consume propellant to counteract atmospheric drag (the decay at an altitude of 400 km can reach the order of 2 km per month [8]), whereas lunar orbits bear no such burden: mascon and third-body perturbations can be managed actively through orbit design (frozen orbits, choice of

altitude and inclination, and so on), whereas atmospheric drag leaves no room for avoidance and fluctuates with the solar cycle.

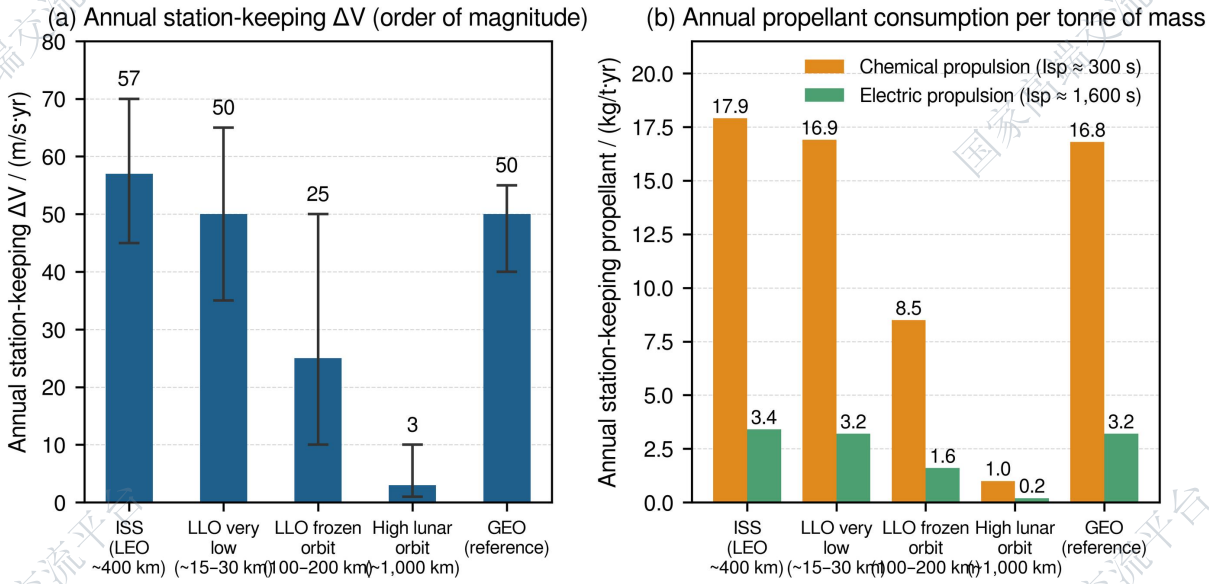


Fig. 5. Comparison of orbit-maintenance costs: (a) order of magnitude of annual station-keeping velocity increment; (b) annual propellant consumption per tonne of mass (calculated in this paper)

The feasibility of a near-Moon orbital platform depends first of all on the energy cost of orbit maintenance. A common misconception is that maintaining an under-stable low lunar orbit (LLO) is expensive because of the perturbations from the Moon's non-spherical gravity field (mascons). For example, the Chang'E-2 mission did increase its orbit-maintenance propellant consumption because its orbit altitude was lowered from 200 km to 100 km. However, quantitative analysis shows that even the "high" LLO maintenance cost is still low in absolute terms.

An orbit-maintenance analysis for an LLO mission shows that, over a mission period of 365 days, 12 orbit-maintenance maneuvers were performed, consuming a cumulative propellant mass of about 6.658 kg (the propellant being water). The propellant consumption of each maneuver was between 0.33 kg and 0.73 kg. For a typical orbiter platform, this means that the annual maintenance propellant consumption is only of the order of a few kilograms. If an electric propulsion system is used, the specific impulse is markedly higher, and propellant consumption can be reduced further. This makes a meaningful comparison with the maintenance cost of satellites in low Earth orbit. Satellites in low Earth orbit must continuously raise their orbits against atmospheric drag, and their annual propellant consumption is often of the order of tens of kilograms. In terms of propellant consumption per unit mass, maintaining a near-lunar orbit is no more expensive than maintaining an Earth orbit, contrary to the intuitive impression that "lunar orbit maintenance is costly". (This comparison depends on the mass and altitude of the specific spacecraft; the annual propellant per tonne in Table 4 should be taken as the standard.)

3.2 Ejection Kinematics and Orbit Departure

When the platform cruises to the designated delivery window, the items M_p loaded in the spindle-shaped payload capsule are ejected backward (retrograde direction) or forward (prograde direction) at a relative velocity V_{rel}. (Convention in this paper: "backward/retrograde" means ejection opposite to the flight direction of the platform; that is, to lower the orbit of the cargo so that it falls toward the lunar surface,

it must be ejected backward.)

The velocity vector of the item after ejection becomes:

$$V_{\text{cargo}} = V_{\text{platform}} + V_{\text{rel}} \tag{2}$$

With retrograde ejection (V_{rel} opposite in direction to V_{platform}), the perilune R_{p} of the item's orbit will fall below the lunar surface:

$$R_p = a(1 - e) \leq R_m \tag{3}$$

The item falls freely along the elliptical transfer orbit. Because the Moon has no atmosphere, the descent trajectory is determined entirely by an unperturbed Kepler orbit and the mascon gravity field, with no capricious crosswind interference, and the delivery impact-point accuracy can be controlled to within the order of 100 m. After correction through long-term, repeated blind deliveries in orbit, a precise model at the meter level may be established. Note: in the ideal two-body model the trajectory and altitude are predictable, but the actual impact-point dispersion is still affected by initial-state errors, platform attitude/ejection errors, the higher-order lunar gravity field, the target terrain, and the geometry of the lunar-surface receiving area. The accuracy requirements must further be discussed by direction (estimated for a 100 km circular orbit with half a revolution of flight after ejection): along the track, a 1 m/s ejection velocity error causes a deviation of about 11 km; across the track, the first-order deviation caused at perilune by an out-of-plane velocity error at the ejection point is zero, and the main contributions come from errors in determining the orbital plane and the Moon's rotation; and what decides success or failure is the vertical direction: the sensitivity of the perilune altitude to the ejection velocity is about 4.2 km/(m/s) (Appendix B, item (8)), that is, an ejection velocity control accuracy of 1% (0.23 m/s) gives a perilune altitude deviation of about 1 km, far greater than the meter-level vertical tolerance of the long-slope entry funnel; to hold the deviation to about 10 m, the velocity error must be reduced to about 2.4 mm/s. The engineering goal of "blind delivery + post-hoc calibration" therefore cannot necessarily satisfy the model requirements; with existing technology, the payload capsule may still need to be equipped, during the half-revolution of flight after ejection (about 1 h), with mid-course correction and terminal guidance based on relative navigation (correction magnitude $\Delta V \approx$ 1–5 m/s, about 0.3–1.7 kg/t of chemical propellant, I_{sp} = 300 s). This requirement shifts part of the lander's navigation complexity onto the payload capsule, but no high-thrust engine or landing legs are needed. The long-slope capture scheme additionally requires a terminal guidance window (about 50 km before the entrance, about 30 s) with $\Delta V \approx$ 2–5 m/s, so that the total guidance ΔV budget is about 3–10 m/s (about 1.0–3.4 kg/t, I_{sp} = 300 s), with a go-around capability reserved (see Section 4.2.3(6)).

From the standpoint of energy economics, landing on the Moon and taking off again constitute the most costly link in the entire transportation chain. Performing a soft landing on the lunar surface from low lunar orbit requires cancelling an orbital velocity of about 1.7 km/s and overcoming gravity losses during landing; taking off from the lunar surface to return to orbit requires regaining a velocity increment of about 1.7 km/s. This does not yet include the propellant reserve needed for precise control in the final stage of landing. A concrete calculated example illustrates the order of magnitude of this penalty. Early NASA mission analysis documents show that for the braking phase from the Earth–Moon transfer orbit to a lunar surface landing, the velocity-increment requirement is about 2,480 m/s and the required propellant mass is about 52% of the initial mass. For a landing stage with an initial mass of 913 kg, this means that 479 kg of propellant is used solely for a one-way landing.

If this cost is multiplied by the total mass of materials required for lunar development, the conclusion is clear: with the lunar surface as the base for delivering materials, every kilogram of the spacecraft body must bear the "energy tax" of landing and re-takeoff; with near-lunar orbit as the delivery harbor, the spacecraft's receiving and transferring of materials involves only orbital maneuvers, and the energy cost falls by orders of magnitude (for platform-side propellant only; the construction cost of the lunar surface long-slope deceleration facility is counted separately, see Section 3.7).

If cargo adopts the "deceleration and delivery mechanism" of "circumlunar platform – spindle-shaped ejection capsule – long-slope electromagnetic deceleration capture", one-way continuous delivery will greatly reduce energy expenditure (on the platform side), and the cargo itself can even assume the role of a momentum-exchange load and become "propellant"; through careful calculation and regulation, platforms in lunar orbit moving prograde or retrograde with respect to the Moon can be driven step by step to change their courses.

3.3 Platform Momentum Compensation and Energy-Level Conversion (Orbital Energy Conversion)

This section discusses an inter-platform cargo kinetic-energy exchange system that, in the sense of ideal momentum exchange, markedly reduces propellant when two-way logistics are balanced: let cargo of ejected mass M_{p} produce a momentum recoil on a platform port of mass M_{plat}. The velocity increment ΔV_{plat} gained by the platform is:

$$\Delta V_{\mathrm{plat}} = -\frac{M_p V_{\mathrm{rel}}}{(M_{\mathrm{plat}} - M_p)} \tag{4}$$

- **Retrograde ejection of cargo:** the platform gains a prograde ΔV_{plat}, and its orbit rises (orbit raising);
- **Prograde ejection of cargo:** the platform gains a retrograde ΔV_{plat}, and its orbit lowers (orbit lowering).

The platform port can use the momentum difference between the periodic receipt of cargo ships from Earth (which bring impulse) and the ejection of cargo toward the lunar surface (which transfers part of the impulse), cycling and regulating within a specific orbital altitude interval just like an "electron energy-level transition". It should be clarified that a current cargo ship docks co-orbitally with the platform after its own LOI braking, so its net velocity impulse on the platform is approximately zero and it does not "bring impulse". In a modular-combination mode, because the platform mass will be much greater than the cargo-ship mass, under a certain inertia it can withstand brief differential-speed berthing. It should additionally be noted that what can really offset the recoil of ejection toward the lunar surface is cargo ascending from the lunar surface: cargo launched electromagnetically from the lunar surface with a perilune speed of about 1.70 km/s rises along a transfer ellipse and has a speed of about 1.610 km/s at the 100 km apolune, 23 m/s slower than the platform; capture of this cargo by the platform at that point is equivalent to applying an impulse of equal magnitude and opposite direction to the recoil of ejection toward the lunar surface. Therefore: (1) when the descending and ascending masses are equal, the net change of the platform orbit is zero, forming a momentum closed loop with the electromagnetic ejection of Section 4.7; (2) when early logistics are dominated by descent, the net recoil is $\Delta V_{\mathrm{plat}} \approx 23\ \mathrm{m/s} \times M_{\mathrm{p}}/(M_{\mathrm{plat}} - M_{\mathrm{p}})$: with $M_{\mathrm{plat}} = 200$ t and $M_{\mathrm{p}} = 1$ t, each tonne of descending cargo raises the platform speed by about 0.12 m/s, and 1,000 t delivered per year accumulates to about 115 m/s, far greater than the annual maintenance level of about 25 m/s, which must be compensated by electric

propulsion or equivalent means, with a required propellant mass of about $M_p \cdot 23/(I_{sp} \cdot g_0)$, about 1.2 kg/t at I_{sp} = 2,000 s, independent of platform mass. The early-stage ejection that ignores inclination is therefore not one that "needs almost no propellant", but one that needs "about 1–2 kg of electric-propulsion propellant per tonne of cargo", which tends to zero as the proportion of ascending logistics rises. But we know that the early stage of lunar construction will necessarily be "extensive": the materials entering the Moon will far exceed the "lunar-made" products sent out after refining, and the phenomenon of "imports" exceeding "exports" will certainly persist for a considerable period. This paper deals precisely with the early to middle stages of lunar construction, and for the net gain this propellant compensation is still "worth spending".

> Discussion of compensation methods for orbit raising: (1) use the tilted sail surface of a solar sail so that radiation pressure produces a component opposing the flight direction, thereby lowering the orbit, but the acceleration is small (estimated for a 1 t platform, 1,000 m² of sail area, and ideal efficiency, about 10^{-5} m/s² in order of magnitude, at most 0.9 m/s per day); (2) continuously capture slower cargo approaching the platform from lunar surface electromagnetic launch, so as to lower the orbit continuously, but this requires high scheduling capability and is feasible only locally in the early stage; (3) convert this increment into receiving, by technical means at the far-lunar end of the orbit, low-momentum items from Earth, or delivering high-momentum items needed by Earth (unloading and transferring cargo), thereby lowering the orbit.

3.4 Environmental Safety and Mobility

The safety of orbital residence comes from the single quality of being "mobile": there is no moonquake coupling; meteoroids can be warned of and evaded; during an SPE, the Moon-blocking window and a storm shelter can be used (during an SPE the storm shelter should be primary and blocking by the Moon secondary); and the platform can also change orbit as a whole to adjust the dwell time within the blocked region. Lunar surface facilities are fixed targets, whereas orbital facilities are mobile bodies. This corresponds one-to-one with the mitigation of the lunar surface hazard list of Section 2.3.

3.5 Advantages for Astronomical Observation and Sky Surveys

Telescopes on the lunar surface are limited by horizon blocking (half the celestial sphere, and a narrower field of view inside craters), by lunar dust settling, and by the large day–night temperature difference of the 300 K class and the resulting structural thermal deformation; an observatory in lunar orbit, by contrast, can survey the whole celestial sphere, is free of dust and extreme thermal cycling (the alternation of day and night is short), and the Moon itself can serve as a natural shield against Earth's radio-frequency interference (RFI); lunar orbit and the far-side sky region are widely recognized as among the best windows for low-frequency radio astronomy [40, 41]. A distinction must be made: ground stations on the far side can receive shielding by the Moon at all times, whereas an array in lunar orbit is shielded only on the arcs where it passes behind the far side (depending on the orientation of the orbital plane, at an altitude of 100 km up to about 39% of the orbital time), but lunar surface stations can provide a stable large foundation and fixed long-baseline geometry. Far-side stations (such as LCRT [41]) and orbital arrays can be complementary, and an interferometric array of a cluster in lunar orbit can return data after observation on the far side to achieve a nearly all-sky low-frequency radio survey [40]. For some specific scientific objectives, the stable attitude and wide-field scanning capability of a far-lunar-orbit platform for optical surveys is also markedly superior to fixed stations on the lunar surface (lunar glass and coronagraph schemes have also been studied [46]).

3.6 Relay Hub and Logistics Efficiency

Lunar orbit is the geometric hub of Earth–Moon logistics: a cargo vessel departing from Earth need only complete the Earth–Moon transfer (TLI ≈ 3.1 km/s) and lunar orbit braking (LOI ≈ 0.9 km/s) to reach the platform port, without paying 3.7–3.9 km/s for "going down and flying back up"; personnel and materials can be transferred between cabins "smoothly" at the platform port (for one-time cargo, the platform avoids having to provision a complete lunar-surface return stage for that batch of cargo; for reusable systems that must return from the lunar surface to orbit, the corresponding ascent ΔV must still be paid). As required, the platform port can also be deployed in a more distant "pseudo-synchronous region" and in frozen orbits, using berthing at the eccentric end to reduce ignition consumption (Appendix B). The lunar-orbit relay design thus provides a low-cost, high-throughput, low-risk logistics backbone for lunar development and opens a continuous channel for two-way exchange of materials between Earth and the Moon.

Comparison with the NRHO scheme: entry into an NRHO (perilune altitude of about several thousand kilometers) requires a lower velocity increment and provides continuous communication with Earth, which suits it as a relay and communication node for Earth–Moon traffic [48]; but it is too far from the lunar surface to support the low-orbit ballistic delivery and electromagnetic ascent of this paper (both require the platform altitude to be tens to hundreds of kilometers). The NRHO and the low-lunar-orbit platform port are therefore not competitors: the former is oriented to relay and the latter to logistics coupling with the lunar surface, and they should be planned together at the system level.

Table 5. Comprehensive comparison of the lunar-surface paradigm and the lunar-orbit paradigm

Dimension (preliminary system comparison)	Lunar-surface paradigm	Lunar-orbit paradigm (Lunar Orbital Port)
Energy cost	Landing 1.9 + departure 1.85 km/s (71.6% propellant for a round trip)	LOI 0.91 km/s + annual maintenance of 1–50 m/s
Technical risk	Soft-landing success rate ≈ 50%, with failures concentrated in the powered-descent phase	Rendezvous and docking technology is mature; no landing phase
Safety	Four hazards: moonquakes, meteoroids, radiation, and lunar dust	Moonquakes and meteoroids can be evaded or mitigated; radiation is of the same order as on the surface and requires built-in shielding; no lunar dust in lunar orbit
Observation	Half the celestial sphere, dust contamination, thermal cycling	Whole celestial sphere, dust-free, stable attitude; radio silence only on far-side arcs, but complementary to stations
Logistics	First-order lander mass estimate for 1 t of payload of about 2.86 t; structure, thermal control, and redundancy must be added in practice	Ballistic delivery requires only 1.01 t per tonne (ΔV ≈ 23 m/s) (some limitations and solutions in Section 3.7)
Expandability	Facilities fixed on the lunar surface; expansion constrained by transport and terrain	Modular cluster platforms that are maneuverable, can fly in formation, are recoverable, and are distributed
Habitability	Requires lunar dust isolation, radiation shielding, and thermal control; surface gravity about 1/6 g	Radiation-shielded floating islands, garden communities, optional artificial gravity, no lunar dust disturbance, expandable into urban clusters

Table 5 gives a direct comparison of the two paradigms using the same set of dimensions. It must be emphasized that the two are not mutually exclusive: an orbital platform is the "front-loaded infrastructure" for finally realizing lunar surface operations, and lunar surface outposts rely on the platform. The former, as the main body, enlarges the spatial range of human activity on the Moon, and

its cluster size and frequency can be configured as required.

3.7 Mass Accounting and Break-Even Analysis

This section performs a break-even analysis using "LLO-equivalent mass" as the unified measure (illustrative parameters, not an engineering conclusion):

(1) Lander direct delivery: each tonne of payload requires c_L = 2.86 t to be assembled in LLO (see Section 2.1).

(2) Ballistic delivery: each tonne of cargo requires, in LLO, 1.0 t of cargo plus a carrier spindle (including the magnet array, guidance module, and propellant; recoverable and reusable); the spindle mass is taken as 0.2 t (author's assumption; if 0.5 t is taken, c_B = 1.5 t), that is, c_B = 1.2 t.

(3) Fixed investment: the platform port mass M_{plat} is taken as 100/200/400 t (author's assumption, with reference to the order of the roughly 420 t of the International Space Station); the lunar surface deceleration facility mass M_{inf} is taken as 50/100/200 t, which must be delivered by landers, each tonne being equivalent to c_L times its mass in LLO. If the lunar surface deceleration facility is shared with the original electromagnetic launch long slope, M_{inf} counts only the incremental retrofit (regenerative converters, energy storage, and entry funnel), and the 50 t column of Table 6 can be used.

(4) The break-even cumulative delivered mass is $N^* = (M_{plat} + c_L \cdot M_{inf})/(c_L - c_B)$; that is, long-term, large-scale, continuous ballistic delivery of materials can yield a positive gain.

Table 6. Break-even cumulative delivered mass N^*/t of ballistic delivery relative to lander direct delivery (c_L = 2.86, c_B = 1.2)

M_{plat} / t	M_{inf} = 50 t	M_{inf} = 100 t	M_{inf} = 200 t
100	146	233	405
200	207	293	465
400	327	413	586

With the representative values (M_{plat} = 200 t, M_{inf} = 100 t), $N^* \approx 293$ t; if the lander can be reused so that c_L falls to 2.0 t, then $N^* \approx 500$ t. This means that at the annual throughput of the order of 1,000 t envisaged in Section 6, about 4 months of deliveries would recover the mass cost of the fixed investment; but for small-scale missions of only tens of tonnes, ballistic delivery is not worthwhile. The limitations of the above analysis are that it does not include operating costs, the maintenance and replacement of long-slope coils and energy-storage equipment, the failure probability, or the platform lifetime, and it does not include the conversion from the Earth LEO starting point (TLI + LOI ≈ 4.0 km/s; with I_{sp} = 450 s, delivering 1 t into LLO requires about 2.5 t in LEO, and with I_{sp} = 360 s about 3.1 t).

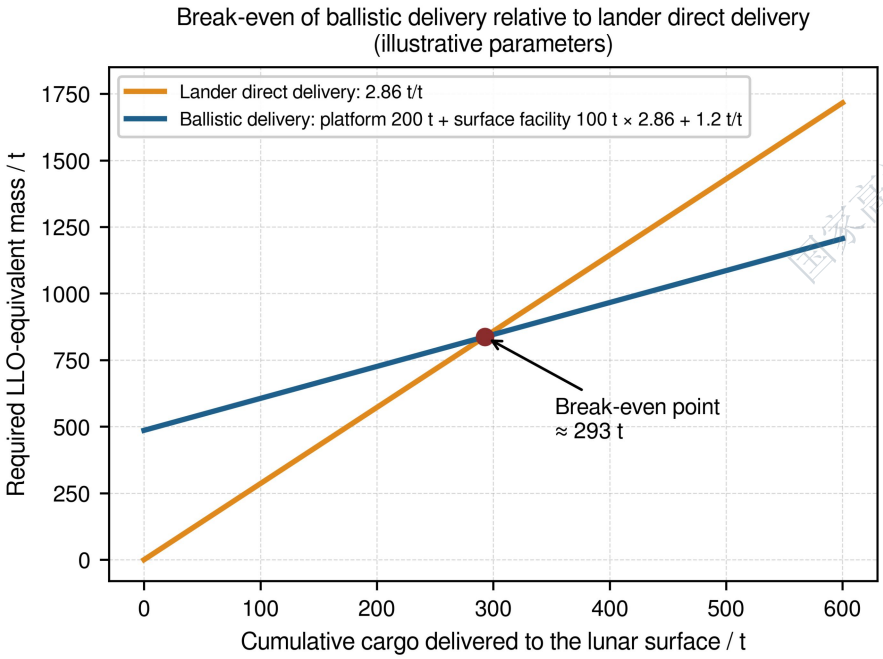


Fig. 6. Break-even of ballistic delivery relative to lander direct delivery (illustrative parameters: M_{plat} = 200 t, M_{inf} = 100 t, c_L = 2.86, c_B = 1.2)

Conclusion: if the cost of the supporting lunar-surface infrastructure for reusable landers is not counted, then treating the construction of lunar-orbit platforms as long-term, deterministically operated infrastructure can greatly reduce the cost of lowering materials to the Moon; whereas for small-batch, low-frequency one-way delivery of materials down to the Moon, with the landing risk set to zero, it is recommended to continue to choose the conventional landing approach. For the shared long-slope case: with M_{plat} = 200 t and M_{inf} = 50 t, N^* ≈ 207 t (Table 6); if the spindle mass is taken as 0.5 t (c_B = 1.5 t), then N^* = (200 + 2.86 × 50)/(2.86 − 1.5) ≈ 252 t, and about 357 t for M_{inf} = 100 t. If the spindle is recovered and reused through upward launch, only its depreciation is counted in c_B, and N^* is lowered accordingly.

4 System Design of the “Lunar Orbital Port”

4.1 Overall Architecture: Platform Ports, Cargo Vessels, and Fixed Delivery Points

The “Lunar Orbital Port” consists of three types of nodes: ① platform ports, large habitation platforms operating in 30–200 km frozen orbits that also serve as delivery, relay, energy, and crew-habitation units; ② ferry vessels, transfer spacecraft shuttling between platforms and between Earth and the Moon, which berth with the platform port frictionlessly in the same direction, keeping their inertia consistent; they can temporarily attach a cabin for cooperative transfer and then detach, helping to switch between far-lunar and near-lunar orbits, and can even be transferred into an Earth–Moon transfer orbit; ③ fixed delivery points, long-slope electromagnetic capture stations on selected flat approach corridors on the lunar surface (converted from the original electromagnetic launch long slope and operated in reverse, comprising an entry funnel, a high-speed regenerative braking section, a gentle-slope docking section, and an entrance platform), which brake regeneratively in sections along the track and recover electric energy in order to receive cargo delivered ballistically. The three form a closed loop of “circumlunar platform – spindle-shaped ejection capsule – long-slope electromagnetic deceleration capture” (Fig. 7).

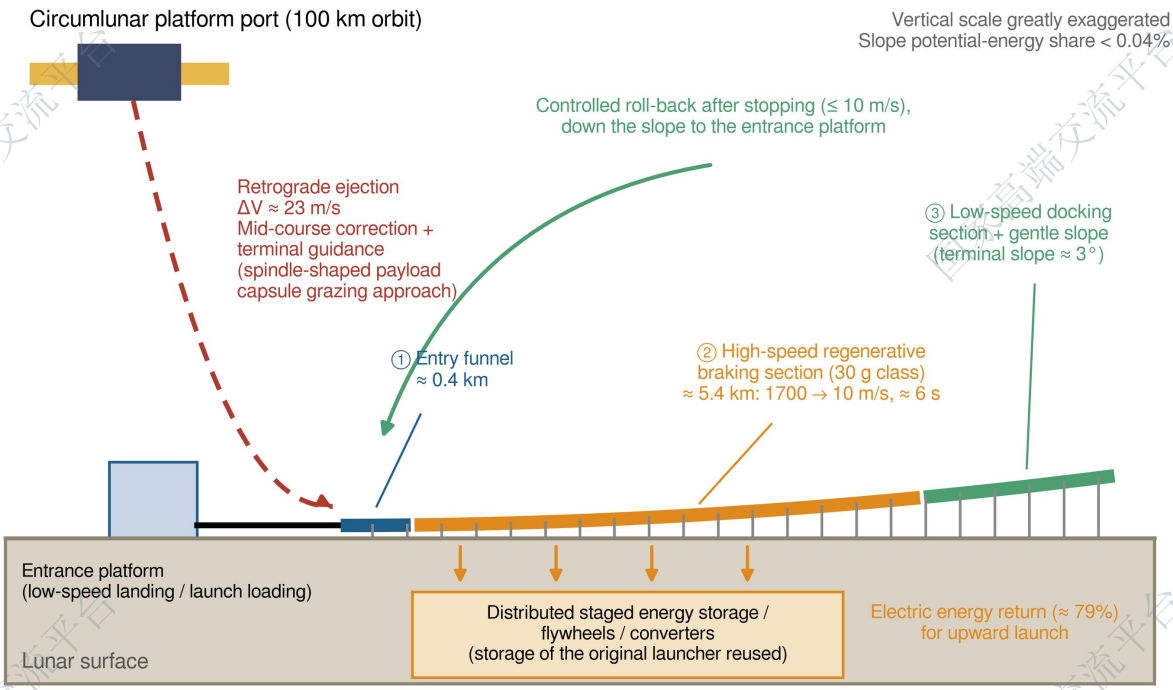


Fig. 7. Conceptual schematic of the "circumlunar platform – spindle-shaped ejection capsule – long-slope electromagnetic deceleration capture" delivery system (vertical scale greatly exaggerated)

4.2 Delivery Scheme: "Circumlunar Platform – Spindle-Shaped Ejection Capsule – Long-Slope Electromagnetic Deceleration Capture"

4.2.1 Orbital Effects of Cargo Ejection

The platform port uses the ejection of cargo as one of its means of orbit maintenance and thus has a dual function: delivery of materials and momentum management. Taking the direction of the platform's instantaneous velocity as the reference, retrograde ejection gives the platform a prograde recoil and tends to raise the orbital energy, while prograde ejection gives the platform a retrograde recoil and tends to lower the orbital energy. The actual change of the orbital semi-major axis also depends on the ejection point, the ejection angle, and the Moon's non-spherical gravity field. The orbital evolution differs when the direction is reversed; see Section 4.3. By alternating ejections prograde and retrograde with respect to the Moon, the platform port can, in the ideal case, achieve partial orbit control without consuming additional dedicated propellant, but practical factors such as the energy consumption of the ejection mechanism, the mass loss of the cargo, and the structural loads on the platform must be included. The orbital balance of the platform can rely on two means: capturing cargo ascending from the lunar surface (see Sections 3.3 and 4.7) and electric-propulsion compensation; for the direction of orbital evolution see Section 4.3. The ejection time and angle parameters can only compensate timing/phase deviations, and vertical deviations must be eliminated by mid-course correction and terminal guidance (see Section 4.2.2). This paper discusses only in simple terms the flight attitude with inclination ignored, and actual operation should also begin with low-mass objects and advance step by step to the tonne class. An intelligent scheduling system can be established to analyze the kinetic-energy state of each spacecraft and allocate resources carefully, ensuring that the process of "cargo descent – platform orbit change" proceeds smoothly and in order.

4.2.2 Ballistic Model and Deceleration Design

Taking 30–100 km at the very near-Moon end as the suitable delivery distance, the model assumes that

the platform operates in a 100 km circular orbit (speed 1.633 km/s) and ejects a 1 t item at a retrograde velocity increment of about 23 m/s, so that its perilune falls at the entrance of the long-slope capture station; thereafter the item falls freely under lunar gravity alone (the lunar surface is an ultra-high vacuum with no aerodynamic drag). From the vis-viva equation, the touchdown speed is about 1.70 km/s, and this speed is predominantly horizontal (grazing slope entry, vertical component ≈ 0). The total impact kinetic energy of the 1 t item is about 1.45 GJ, equivalent to about 346 kg of TNT; this kinetic energy is regeneratively braked in sections by the long-slope electromagnetic installation and recovered, and the cargo finally completes a soft landing at the entrance platform at low speed or at rest. Specifically, electromagnetic energy absorption on a straight track several kilometers long (mainly long-stator linear-motor generator braking, supplemented by eddy-current braking) converts the kinetic energy into electric energy, which is fed back into the energy-storage system of the launcher (reverse charging) [63–67], while the low-inclination slope of the track converts part of the kinetic energy into potential energy of height, the two acting in concert to decelerate the cargo; until physical test data are obtained, this paper calls it "controlled ballistic delivery" and does not call it a verified soft landing. The lunar surface is an ultra-high vacuum, there is no aerodynamic interference while the ejected object falls, and the parameters are extremely simple; the establishment of the capture model depends mainly on local variations of the Moon's gravity field. Although its dynamical environment lacks the major uncertainties of Earth's atmospheric wind fields and aerodynamic drag, the Moon's higher-order gravity field, the terrain, and initial errors will still produce impact-point dispersion, so Monte Carlo error propagation and measured calibration are needed, and a precise "capture impact-point model" [3] can be established from a gravity field model (such as GRGM900C [3]) and a small number of calibration shots. To eliminate the time variation of the mascons (tides) and pointing errors, multiple rounds of blind-delivery calibration are still needed to improve practical accuracy.

The core idea of the scheme is to operate the original electromagnetic launch installation on the lunar surface in reverse: the installation was originally used to accelerate lunar surface cargo electromagnetically in pulses along a straight track several kilometers long with an inclined slope to about 1.70 km/s and throw it into lunar space [35, 36, 63]; in reverse operation, the same long track is switched to braking/generating mode to capture cargo arriving from lunar space in grazing flight. The process is as follows: ① after precise guidance close to the lunar surface, the object enters the track entrance transition section at a horizontal grazing speed of about 1.70 km/s; ② on the straight long-slope track several kilometers long, deceleration is carried out by two principles: first, electromagnetic energy absorption by the track (long-stator linear-motor generator braking and eddy-current braking), converting kinetic energy into electric energy and charging it back into the energy-storage system of the launcher; second, using the low-inclination slope of the long track itself to convert part of the kinetic energy into potential energy of height difference; ③ after the object's speed has been reduced to zero, it enters the terminal capture section; ④ the object is then allowed to slide slowly down the track slope in a controlled manner, continuing to dissipate energy by generating power as it slides down and absorbing the remaining potential energy (also reverse charging), and finally returns at low speed or at rest to the entrance of the launcher and is then guided into the unloading area, completing a smooth landing.

Cargo form and interface design (corresponding to the engineering constraints of Section 4.2.2): to satisfy the requirements of electromagnetic braking and track contact, the cargo should carry an electromagnetic coupling interface of aluminum/copper or similar, serving at the same time as a

structural load-bearing layer, with the payload wrapped in a shock-absorbing outer layer (metal foam/honeycomb); the outer shape should be designed as a barrel-cylinder body with conical/ovoid ends, which facilitates low-friction clamping and guidance centering by roller carriages/magnetic levitation cradles and also benefits the uniformity of magnetic-field coupling and the structural load distribution; the track entrance section should use roller carriages together with electromagnetic levitation cradles, so that the cargo enters in a low-friction/frictionless manner and high-speed contact shock is avoided. The scheme does not mean that a free-flying object can "crash into" the track directly without terminal guidance: entrance capture is itself a high-risk critical link and must first be verified through small-mass tests.

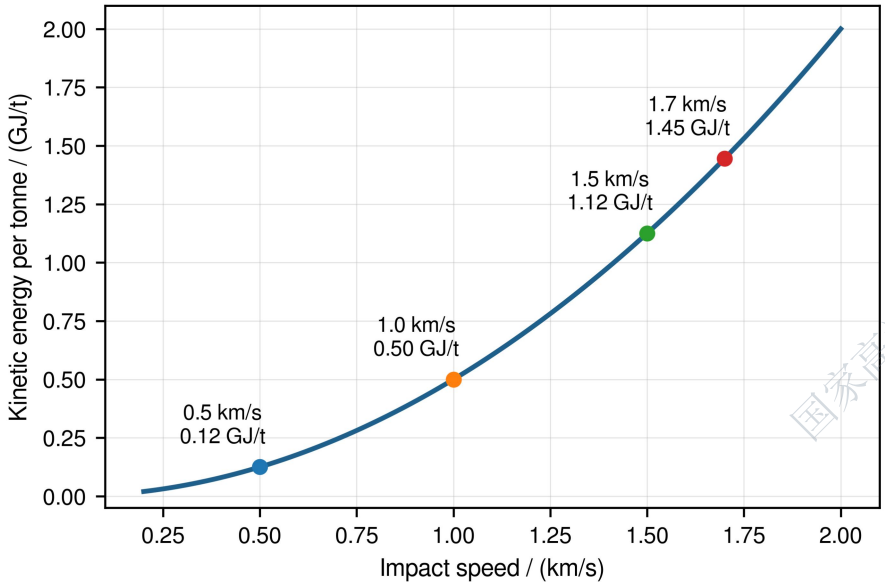


Fig. 8. Impact energy of an object in the near-vacuum environment of the lunar surface

On the premise of accurate delivery, Table 7 gives the mean deceleration g-load for different energy-absorption length scales: the "energy-absorption length scale L" in the table is the effective deceleration stroke of the long slope; the payload capsule is assumed to be a spindle-shaped reinforced capsule loaded along the track axis, with the cargo within the tolerable range of the vibration-isolated mounts inside the capsule; the kinetic energy of grazing incidence is predominantly horizontal and is absorbed in sections along the axis by the long-slope electromagnetic installation and recovered (Fig. 9a, Fig. 11).

Table 7. Energy-absorption length scale versus mean deceleration g-load (touchdown speed 1.70 km/s, vacuum grazing, approximately constant deceleration)

Energy-absorption length scale L / km	0.2	0.5	1	2	5
Mean deceleration g-load / g (ideal constant-deceleration model)	≈ 739	≈ 295	≈ 148	≈ 74	≈ 30
Impact kinetic energy of a 1 t item / (kg TNT equivalent)	346	346	346	346	346

Note: The g-load is calculated as $a = v^2/(2L)/g_0$; in actual design the peak g-load is determined by the regenerative braking force limit and the jerk ramp and is about 9% higher than the mean (Table 9), and this paper uses the mean as an approximation.

As the above model data show, ignoring the projected area of the object, for a 1 t cargo falling freely from an altitude of 100 km, even if only a minimum mean deceleration of about 30 g is allowed, an energy-absorption length scale of kilometers is required, which indicates that the engineering difficulty of receiving a direct impact at the 1.70 km/s level is extremely high; it cannot rely on consumable cushioning materials (each tonne of cargo would require 48–145 t of one-time energy-absorbing material, Appendix B(9)), and should turn instead to long-slope electromagnetic sectional regenerative

braking that is reusable and energy-recovering, verified step by step through ground-based scaled electromagnetic/eddy-current deceleration-track tests and lunar-surface suborbital tests.

4.2.3 Long-Slope Electromagnetic Deceleration Capture System

(1) Principle: operating the launcher in reverse. The original electromagnetic launch installation consists of a straight acceleration track several kilometers long, staged pulsed coils (or linear synchronous motors, LSM), and distributed energy storage: during launch, the stored energy is converted into payload kinetic energy by pulsed discharge. This scheme uses it in reverse in the spirit of "time reversal": the payload capsule grazes into the entrance tangentially to the track at a speed of about 1.70 km/s, the coils of each stage are switched to generating (regenerative braking) mode and draw energy from the magnetic field of the payload capsule, converting the kinetic energy stage by stage into electric energy in the storage units of each stage, which is then used for the next upward launch. This idea is not entirely new in physical terms: the design of a mass driver itself contains a deceleration section, which decelerates the empty "bucket" after unloading and recovers its energy, the total length being the sum of the acceleration and deceleration sections [55]; shipboard electromagnetic aircraft launch systems use disk alternators for energy storage and linear-motor propulsion [56]; the new generation of electric arresting gear uses large induction motors in conjunction with energy-absorbing devices to decelerate landing aircraft in a controlled manner [57]; and the fact that a linear motor has both motoring and generating (regenerative) operating states is a standard conclusion of electrical machine theory [60]. The vacuum, low gravity, and absence of atmosphere on the Moon mean that neither airtight tubes are needed nor does the payload capsule suffer aerodynamic drag or aerodynamic heating, which is favorable to such installations. By function, the capture working area is divided into four parts: the entry funnel, the high-speed regenerative braking section, the low-speed docking and gentle-slope section, and the entrance platform (Fig. 7).

(2) Accounting for the three deceleration mechanisms. Let the total mass of the payload capsule (cargo plus spindle) be m and its speed on entering the track v_0 = 1.70 km/s; the kinetic energy per unit mass to be dissipated or recovered is then $v_0^2/2$ = 1.445 MJ/kg (that is, 1.445 GJ/t, about 401 kWh/t). The accounting conclusions for the three mechanisms are as follows.

① Electromagnetic energy absorption by the track (main mechanism): realized by actively controlled LSM regenerative braking, for which the braking force $F = m \cdot a$ can be output constantly at the set g-load limit, essentially independent of speed; the mean g-load is $n = v_0^2/(2L \cdot g_0)$ (Table 7, Fig. 9a). With a total mass of 1.2 t and a limit of 30 g, $F \approx 353$ kN; at a thrust areal density of the order of 150 kPa for permanent magnets/superconducting magnets, the required effective thrust area is about 2.4 m², which is below the limit allowed by the magnetic pressure of a 1 T field (about 0.4 MPa) and can be provided by the magnet arrays on both sides of the payload capsule. The instantaneous mechanical power $P = F \cdot v$ is about 574 MW initially, borne successively by hundreds to thousands of coil stages, each of which handles only energy of the order of 1.7 MJ.

② Passive eddy-current braking (backup mechanism): a conductor plate (aluminum or copper) moving in a magnetic field generates eddy-current drag, requires no power supply, and is fail-safe. However, according to the Reitz model [58], the eddy-current drag first increases and then decreases with speed, with its peak near a characteristic speed v_c; for $v \gg v_c$, $F \propto 1/v$, and the upper limit of the dissipable power is about $2F_{pk} \cdot v_c$. To dissipate 1.7 GJ in about 6 s (average power about 280 MW) requires $F_{pk} \cdot v_c \approx 140$ MW; taking v_c = 5 m/s gives $F_{pk} \approx 28$ MN, which at a magnetic pressure of 0.4 MPa requires an

effective area of about 70 m² and is difficult to achieve (Fig. 10b). Eddy-current braking is therefore suitable only for the low-speed section (below about 100 m/s), for loss-of-power protection, and for roll-back speed limiting, and not as the main means of decelerating from 1.7 km/s.

③ Conversion of kinetic energy to potential energy on the slope (auxiliary mechanism): with the lunar g_m = 1.624 m/s², absorbing the kinetic energy entirely by raising would require a rise of $v_0^2/(2g_m)$ ≈ 890 km; for a track 6 km long, even if placed vertically it could absorb only about 0.67% of the kinetic energy, and a 3° gentle slope only about 0.035% (Table 8, Fig. 9b). Its gravitational deceleration is only $g_m \cdot \sin\theta$, about 0.085 m/s² at 3°, negligible relative to the main braking deceleration of about 294 m/s² (Fig. 10b). The slope therefore cannot take on the main deceleration task, and its value lies in the low-speed stage: (i) from 10 m/s, a 3° gentle slope can bring the payload capsule naturally to a stop within about 590 m by gravity alone, and this holds equally in the event of a loss of power; (ii) after stopping, the payload capsule rolls back down the slope on its own without traction, with its speed limited by LSM regenerative braking; the potential energy recovered during roll-back is only about 0.24 MJ (0.07 kWh) per capture and is negligible.

Table 8. Contribution of kinetic-to-potential energy conversion on the slope (6 km straight slope, v_0 = 1.70 km/s, g_m = 1.624 m/s²)

Slope θ	Rise h / m	Potential-energy gain as fraction of kinetic energy	Gravitational deceleration $g_m \cdot \sin\theta$ / (m/s²)	Gravity stopping distance from 10 m/s / m	Gravity stopping distance from 20 m/s / m
3°	314	0.035%	0.085	588	2,353
10°	1,042	0.117%	0.282	177	709
30°	3,000	0.337%	0.812	62	246
90°	6,000	0.674%	1.624	31	123

Note: Potential-energy fraction = $g_m \cdot h/(v_0^2/2)$; gravity stopping distance $s = v^2/(2g_m \cdot \sin\theta)$. Full absorption by potential energy would require a rise of about 890 km.

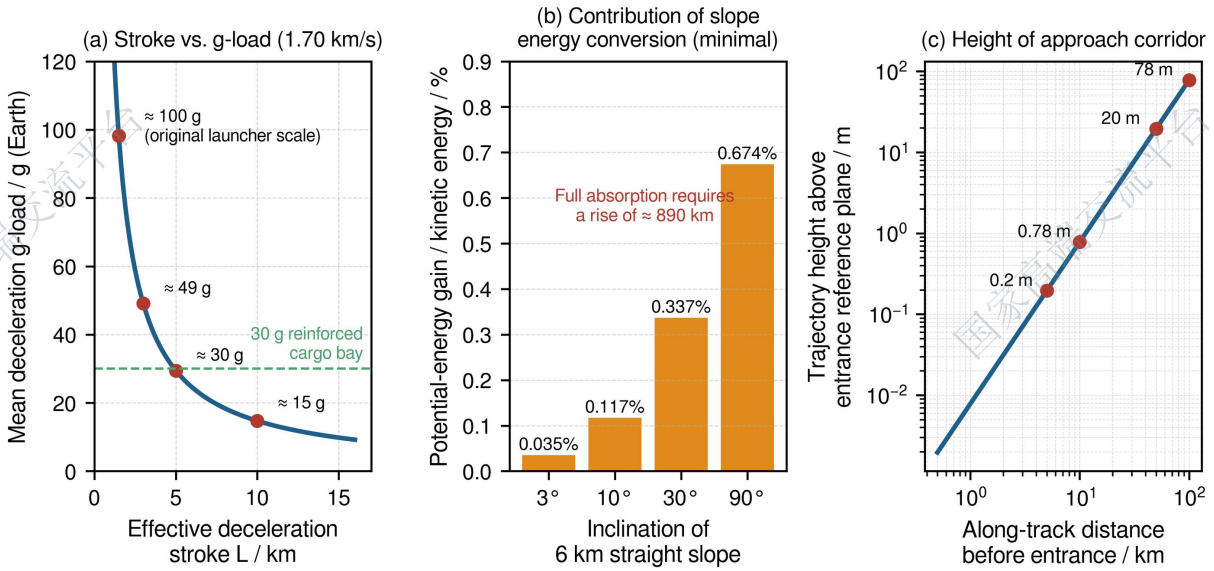


Fig. 9. Design space of long-slope capture: (a) deceleration stroke and mean g-load; (b) contribution of conversion to potential energy on a 6 km straight slope; (c) height of the ballistic trajectory above the entrance reference plane in the approach corridor (calculated in this paper; formulas in Appendix B(15) and (18))

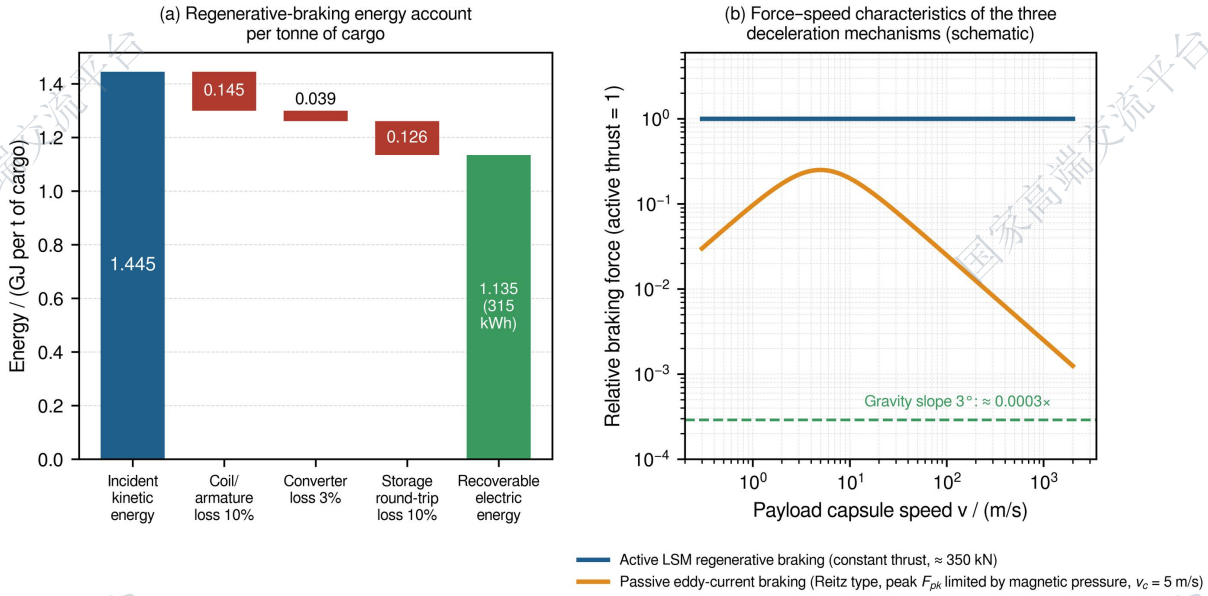


Fig. 10. (a) Regenerative-braking energy account per tonne of cargo; (b) force–speed characteristics of the three deceleration mechanisms (schematic; the eddy-current braking peak is taken as 0.25 of the active thrust)

(3) Overall configuration and baseline example. ① Entry funnel (about 0.4 km): a U-shaped guide channel tapering from a mouth width of ±2 m to ±0.1 m, which passively centers the payload capsule after terminal guidance; if the capsule hugs the wall at the edge of the ±2 m window, the lateral relative velocity is about 8.5 m/s ($v_0 \times 2$ m/0.4 km) and the wall-contact kinetic energy is about 43 kJ, absorbed by crushable bumpers on the nose cone and side edges of the payload capsule. ② High-speed regenerative braking section (about 5.4 km): the payload capsule decelerates from 1,700 m/s to 10 m/s. ③ Low-speed docking section and gentle slope: regenerative braking from 10 to 0 m/s at 0.3 g, completed in about 17 m and 6.8 s. ④ Entrance platform: after rolling back to the entrance, the capsule docks and unloads at a low speed of no more than 0.5 m/s; the spindle can be loaded directly with upward cargo and launched back to the platform by the original launcher (spindle reuse, see Section 3.7).

The longitudinal profile of the track takes the form of a parabolic vertical curve $h(x) = x^2/(2R_c)$, with $R_c = L/\theta_e$; taking L = 6 km and a terminal slope $\theta_e = 3°$ gives $R_c \approx 115$ km, and the normal acceleration required at the entrance is $v_0^2/R_c \approx 25$ m/s² (about 2.6 g), far less than the axial 30 g and available from the levitation force of the payload capsule; the end of the braking section ($x \approx 5.35$ km) is raised by about 125 m, with a local slope of about 2.7°. The vertical radius of curvature of the high-speed section must be sufficiently large (of the order of 100 km or more) to limit the normal g-load, so the slope builds up gradually through the vertical curve rather than rising abruptly at the entrance; the gentle slope does not help the braking itself (see (2)③) and merely creates conditions for the low-speed section and the roll-back.

Approach corridor: a payload capsule ejected by a 100 km platform with a retrograde increment of about 23 m/s descends along an ellipse ($e \approx 0.028$), and at 5, 10, 50, and 100 km along the track before the entrance its trajectory lies about 0.2, 0.78, 20, and 78 m, respectively, above the entrance reference plane (Fig. 9c). If the entrance were at the same height as the perilune, the approach corridor within 10 km would have to be leveled to the sub-meter level, which is not acceptable in engineering; the entrance is therefore raised by $H_p \approx 15$ m (roadbed or elevated structure), so that terrain relief within 10 km before the entrance need only be below about 16 m and below about 35 m at 50 km, which can be satisfied by

selecting a flat mare region.

The simulation results for the baseline example (total payload capsule mass 1.2 t, of which cargo 1 t and spindle 0.2 t; g-load limit 30 g; jerk 60 g/s) are shown in Fig. 11: the braking section is 5.34 km long and lasts 6.24 s, with a mean g-load of 27.6 g and a peak of 30 g; the final braking speed is 10 m/s; the peak power is 574 MW and the mean power 278 MW; the total dissipated kinetic energy is 1.73 GJ (482 kWh). The stopping point is about 5.35 km from the entrance and about 125 m above it; without limitation, the speed on rolling back to the entrance would be about 20 m/s; with the LSM speed limited to 10 m/s, the roll-back takes about 10.3 min (18.5 min at a 5 m/s limit and 7.4 min at 20 m/s).

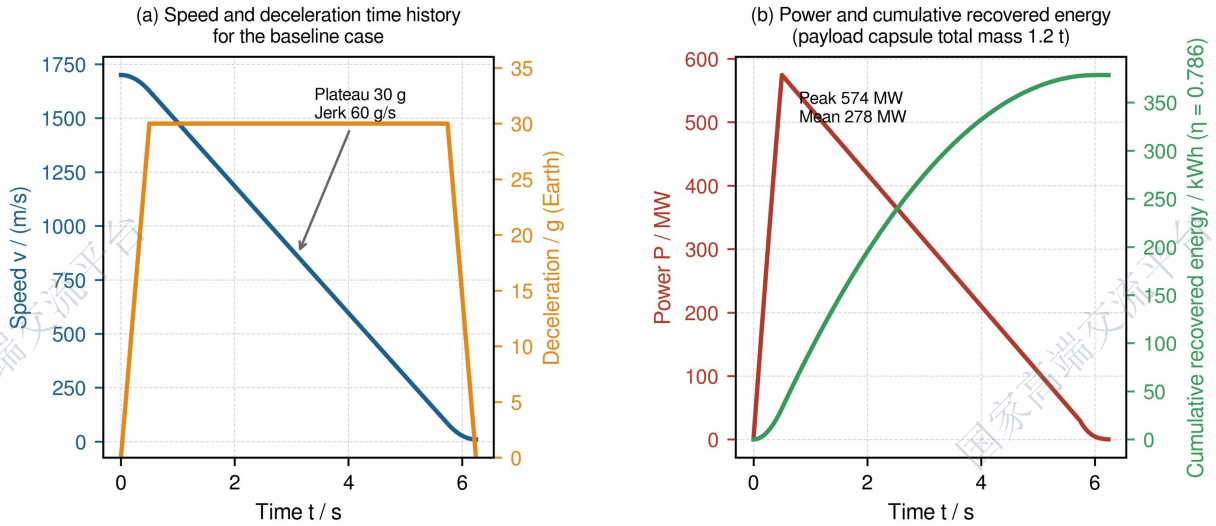


Fig. 11. Time history of the baseline example (1.2 t, 30 g limit): (a) speed and deceleration; (b) regenerative braking power and cumulative recovered electric energy

Table 9. Design space: g-load limit – braking stroke – power (v_0 = 1.70 km/s, braking to 10 m/s, total mass 1.2 t, jerk = 2 × limit per second)

G-load limit / g	Braking stroke / km	Duration / s	Mean g-load / g	Peak power / MW	Mean power / MW	Remarks
15	10.25	12.0	14.4	294	145	Low g-load, longest stroke
20	7.79	9.1	18.9	389	190	
30	5.34	6.2	27.6	574	278	Baseline (this paper)
50	3.37	3.9	43.7	928	439	Corresponds roughly to the 3 km-class original launch track
100	1.90	2.2	77.6	1,712	780	Corresponds roughly to the 100 g, 1.5–1.9 km-class launch track

Note: If the converter peak power is limited to 300 MW, braking at the 30 g limit degrades to constant-power braking in the high-speed section, and the stroke increases to 7.2 km and the duration to 7.6 s.

Table 9 shows that the stroke is approximately inversely proportional to the g-load: the 10 g class needs about 10 km and the 100 g class about 1.9 km (consistent in order of magnitude with the 100 g/1.5 km of the original launcher in Section 4.7). If the original launch track is several kilometers (3–6 km) long, it corresponds to a capture g-load of 50 g to 25 g, and the cargo must be reinforced to this level; carrying humans (≤ 3 g) would require a track length of about 49 km, which is outside the near-term scope of this paper.

(4) Design of the payload capsule (carrier spindle): metal wrapping, shape, rollers, and outer wrapping layer. Regarding "whether the object needs a metal wrapping": the cargo itself does not need

a metal wrapping, but the carrier spindle that carries the cargo does need a metal structure, for four reasons: (i) the aluminum/copper armature plate on the belly of the spindle provides a closed current loop for passive eddy-current braking and levitation, and its thickness must be no less than the electromagnetic skin depth: taking a pole pitch $\tau = 5$ m and $v = 1.7$ km/s, the electrical frequency is $f = v/(2\tau) \approx 170$ Hz and the skin depth of aluminum is about 6.5 mm, so 8–10 mm is taken, covering 1–1.5 m², with a mass of about 22–32 kg; (ii) the magnet array (Halbach permanent magnets or high-temperature superconducting coils) must be fixed to a rigid load-bearing structure; (iii) the metal shell provides the cargo bay with magnetic shielding and thermal equalization, protecting electronic cargo; and (iv) it withstands a quasi-static axial load of about 30 g. The cargo may be non-metallic (lunar regolith bricks, composites, storage tanks, and so on) and is not required to be conductive.

Regarding "shape": in vacuum there is no aerodynamic drag or aerodynamic heating, and a "fluid spindle shape at both ends" has no meaning in fluid dynamics; the constraints on shape come from the guideway and guidance: a slender body of rounded-rectangular or circular cross-section with a length-to-diameter ratio of 3–4 is adopted to match the U-shaped channel and obtain passive pitch stability; symmetric conical heads (half-cone angle 10°–15°) are provided at both ends, the front cone acting as the "probe" of the entry funnel and the rear cone allowing the same spindle to be used in reverse for upward launch, achieving dual use of one spindle (Fig. 12).

Regarding "rollers on the track": at 1.7 km/s rollers are infeasible (rim centrifugal stress, bearing heating, and vacuum cold welding); the high-speed section should use passive electrodynamic suspension (EDS). Inductrack-type Halbach arrays need no power supply, have a levitation onset speed of only a few meters per second, and are fail-safe [59]; Holloman maglev sled tests have reached about 189 m/s (423 mph) on a track with superconducting magnets and copper plates [61], and the conventional sled track at that test range has achieved a land sled speed of 2,885 m/s [62], which indicates the engineering feasibility of guidance and levitation at this speed order of magnitude. Retractable rollers or skids are used only below about 5 m/s (below the levitation failure speed) and in emergencies.

Regarding the "outer shock-absorbing layer": under normal operating conditions, the 30 g axial deceleration is an overall load transmitted along the spindle structure, and an outer layer of foam cannot reduce this load and only adds mass; the truly useful cushioning lies in two places: (i) crushable bumpers on the nose cone and side edges (aluminum honeycomb, with a specific energy absorption of 10–30 kJ/kg, so that 43 kJ of wall-contact energy requires no less than 4.3 kg, and 20 kg is taken in design as margin), used for wall contact in the funnel and off-nominal entry; and (ii) vibration-isolating mounts in the cargo bay, used to limit transient loads (the 60 g/s jerk ramp already reduces the initial shock to the order of about 0.5 s). For the complete energy of 1.73 GJ, consumable energy absorbers would need 58–173 t (Appendix B(9)), so the outer wrapping layer cannot become the main means of deceleration.

Table 10. Key design points of the payload capsule (carrier spindle)

Component	Function	Metal required?	Design recommendation
Shell/load-bearing structure	Load bearing, magnetic shielding, thermal equalization	Yes (aluminum/titanium alloy)	Shell thickness designed for the combined 30 g axial and 2.6 g normal loads; the cargo itself needs no metal wrapping
Armature plate	Eddy-current braking, levitation circuit	Yes (aluminum/copper)	Belly, 8–10 mm, 1–1.5 m², about 22–32 kg
Magnet array	LSM thrust and levitation	—	Halbach permanent magnets (no quench, heavier) or REBCO superconductors (lighter, require cooling and redundancy); thrust area about 2.4 m²

Component	Function	Metal required?	Design recommendation
Levitation and guidance	High-speed support and centering	—	Passive EDS (Inductrack type), levitation onset speed of a few m/s; passive centering by the side walls
Rollers/skids	Low-speed support, emergency	Depends on material	Used only at ≤ 5 m/s; must not be relied upon in the high-speed section
Outer shock-absorbing layer	Protection for off-nominal entry	—	Aluminum-honeycomb bumpers of about 20 kg at the nose cone/side edges; vibration isolation inside the cargo bay; not the main means of deceleration
Shape	Channel matching, passive stability	—	Rounded cylinder, L/D ≈ 3–4, symmetric conical heads at both ends (half-cone angle 10°–15°); no aerodynamic shape needed in vacuum
Guidance/RCS	Terminal guidance, go-around	—	Cold gas or bipropellant; Δ V 3–10 m/s, with go-around counted separately at 1.3–5 m/s
Cargo bay	Payload carrying	Not required	Cargo ≤ 1 t, reinforced for about 30 g; magnetic shielding added for electronic cargo

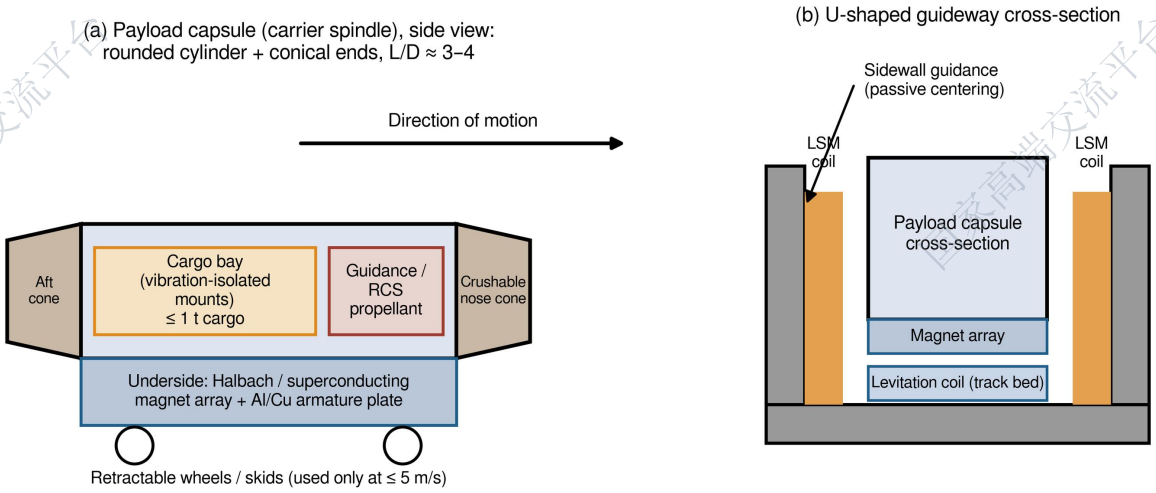


Fig. 12. Schematic of the payload capsule and guideway cross-section: (a) side view of the payload capsule; (b) cross-section of the U-shaped guideway

(5) Energy recovery and reverse charging. The energy chain is: payload capsule kinetic energy → coils/armature (η_1 ≈ 0.90) → converter (η_2 ≈ 0.97) → storage round trip (η_3 ≈ 0.90) → returnable electric energy, with a total efficiency $\eta \approx 0.786$ (author's assumption, corresponding to the typical order of magnitude of existing linear motors, power electronics, and flywheel/capacitor energy storage [56, 60]). On this basis, about 1.135 GJ (315 kWh) can be recovered per tonne of cargo, about 70% of the electric energy required to launch 1 t of cargo upward in Section 4.7 (406 kWh/t ÷ 0.90 ≈ 451 kWh/t) (Table 11, Fig. 10a); that is, with 1 t descending and 1 t ascending, the net electricity consumption of the lunar surface long slope falls from about 451 kWh to about 136 kWh, and when the descending and ascending masses are unequal the accounting is done proportionally. When the total recovery efficiency is taken as 0.6 or 0.9, the returnable electric energy is about 241 or 361 kWh/t, respectively.

Table 11. Energy account for the baseline example (v_0 = 1.70 km/s; per tonne of cargo and per capture of a 1.2 t payload capsule)

Item	Per tonne of cargo / GJ	Per tonne of cargo / kWh	Per capture (1.2 t) / GJ	Per capture (1.2 t) / kWh
Incident kinetic energy	1.445	401.4	1.734	481.7
Coil/armature loss (10%)	0.145	40.1	0.173	48.2

Item	Per tonne of cargo / GJ	Per tonne of cargo / kWh	Per capture (1.2 t) / GJ	Per capture (1.2 t) / kWh
Converter loss (3%)	0.039	10.8	0.047	13.0
Storage round-trip loss (10%)	0.126	35.1	0.151	42.1
Returnable electric energy (78.6%)	1.135	315.4	1.362	378.4

The unrecoverable 21.4% (about 0.37 GJ per capture) is converted into heat, averaging about 70 kJ/m along the 5.4 km track; if the equivalent copper mass of each coil stage is taken as 50 kg (assumption), the temperature rise for a single capture is about 18 K; with 12 captures per day, the average heat load over the whole track is about 52 kW, which can be borne by radiative cooling and the low temperature of the lunar night. The potential energy recovered during the roll-back phase (about 0.24 MJ per capture) is only 0.014% of the total energy and is not accounted for separately. For 1,000 t delivered per year, the kinetic energy to be recovered over the year is 1.45 TJ (about 46 kW on average) and the recovered electric energy is about 315 MWh/a; the recovered electric energy can be fed to the DC bus, supercapacitors/batteries, lunar lava-tube gas filling, or the power grid, for use in the next launch, in control systems, or in auxiliary orbital equipment.

(6) Guidance accuracy, tolerances, and failure modes. Accuracy: from about 50 km before the entrance (about 30 s), relative navigation is carried out using beacons (laser/radio-frequency) at the capture station as the reference, requiring ±2 m laterally, ±1 m vertically, and ±0.3° in pitch/yaw at the funnel mouth; a deviation of the 50 m class is corrected within 25 s, requiring an acceleration of about 0.16 m/s² and $\Delta V \approx 4$ m/s, which together with the mid-course correction of Section 3.2 makes up a guidance budget of 3–10 m/s. The tolerance order of magnitude of this scheme is the meter level, the same as that of the original "cable-net" scheme, but the capture structure is linear, reusable, and free of dust raising.

Go-around: when the go-around decision is made 30 s before the entrance, raising the track by 20 m requires only about 1.3 m/s; a payload capsule that misses the entrance continues to fly along the near-circular ellipse, and after about half a revolution (about 1 h) it can approach again by raising the perilune at apolune with an increment of a few m/s (sensitivity about 4.2 km/(m/s)), so a missed capture does not necessarily end in impact with the Moon, but a flat escape corridor must likewise be reserved downstream of the entrance.

Failure modes: (i) loss of power or converter failure: the sections are isolated, the remaining coils continue braking, and eddy-current braking and the gentle slope act as the last line of defense; if the LSM fails entirely, the payload capsule will shoot out of the end of the track at close to 1.7 km/s, and upstream diagnostics must terminate the approach 30 s before the entrance, with a regolith embankment additionally provided downstream; this is a catastrophic failure and must be guarded against with particular care; (ii) quench of superconducting magnets or demagnetization of permanent magnets: permanent-magnet Halbach arrays avoid quench but are heavier, and superconducting schemes must carry redundant windings; (iii) levitation failure: emergency landing on skids would cause severe damage in the high-speed section, so the levitation must be redundant and self-checked before the entrance; (iv) lunar dust: this scheme has no engine plume and will not raise dust as a powered landing does (Section 2.3.4); the guide channel needs a sintered surface and must be inspected for debris between captures; (v) lunar night: the energy storage, coils, and cryogenic systems must be insulated, and the power supply is described in Section 4.4.

Scope of application and limitations: This scheme is suited to raw materials, structural parts, reinforced equipment, and storage tanks of the 1 t class that can withstand about 30 g, and is not suited to personnel or fragile cargo (the ramp would need to be redesigned with a longer length); integral regenerative braking at the 1.7 GJ/6 s level and long-term operation on the lunar surface have no precedent and must be verified by the step-by-step scaled tests of Sections 6 and 7; the efficiency chain, stage pitch, spindle mass ratio, levitation and magnet parameters, and so on in this section are all author's assumptions used for first-order scale estimates and do not constitute an engineering commitment; in the one-dimensional braking model of this paper, either increasing the electromagnetic braking force or lengthening the track can reduce the g-load, but this result is only a static energy-balance result. Engineering design should further adopt a staged system of "electromagnetic-braking pre-deceleration + eddy-current braking + slope potential-energy recovery + terminal low-speed capture", with peak g-load, recovery efficiency, and cargo integrity as acceptance indicators: exhaustive measures with multiple means acting in concert should be used to dissipate the kinetic energy carried by objects ejected from a high lunar orbit, which are in practice of the tonne class, and if residual speed remains, a cable net and collapsible energy-absorbing bodies may be set up on the lunar surface as a backstop; going further, as infrastructure capability grows to the level of capturing more than a hundred tonnes at low g-load, with the help of guided recoil propulsion, one day living beings could be wrapped in a metal outer shell with multi-stage cushioning layers, cut in grazing flight from lunar space into the long-slope electromagnetic deceleration track, and be intercepted in a controlled manner down to low speed, becoming a unique personnel entry channel on the Moon (an unpowered/low-power personnel soft-landing system, a crewed airport).

4.2.4 Delivery Windows and Throughput

The platform port patrols the Moon with a period of about 1.85–2.13 h, and within each window multiple items can be delivered in turn, with multiple receiving points (long-slope capture stations) provided in the lunar surface projection area of the ground track; for the platform port, ejecting cargo backward is equivalent to expelling propellant and produces a positive orbital maneuver effect (orbit raising), while ejecting forward lowers the orbit (cargo ejected forward does not fall toward the lunar surface; it is designated as inter-platform momentum exchange and used only to adjust the platform orbit or to move to another orbit): delivery is itself orbit change, and logistics and orbit are maintained in a unified way (see Section 4.3). After the accumulation of multiple windows, the platform port restores its nominal orbit through the upward-cargo capture and electric-propulsion compensation described in Section 3.3. In scenarios of high throughput demand, multiple platform ports can be arranged in succession on the same circumlunar line to form a formation for throughput. The time occupied by one capture on a single long slope is about 6 s of braking plus about 10 min of docking and controlled roll-back, far shorter than the platform overhead pass period (about 1.97 h), so the theoretical upper limit of a single station is about 12 items per day (about 4,400 t/a at 1 t per item), and the annual throughput of the 1,000 t class in Section 6 requires only about 3 items per day.

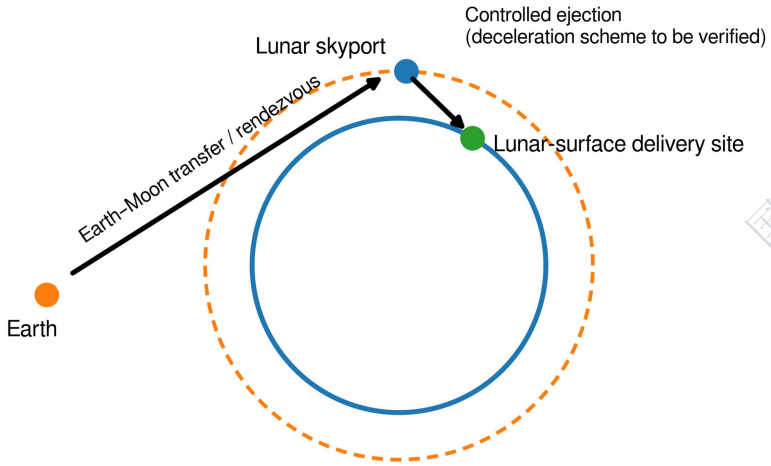


Fig. 13. Framework of the "Lunar Orbital Port": orbital port – ferry spacecraft – lunar-surface fixed point

4.2.5 Optimization of Eccentric Orbits and Solar Energy Acquisition

The circumlunar platform port is set in a non-circular orbit (perilune H_p = 30 km, apolune H_a = 300 km), with the apolune placed in the lunar day hemisphere (the Sun–Moon geometry and orbit precession necessarily change, and continuous optimization of the apolune keeps it fixed in the lunar day hemisphere). According to Kepler's second law, the platform moves slowly and dwells for a long time at apolune, which maximizes the use of solar panels for photovoltaic generation and energy storage (the actual net generation gain must also take into account the solar incidence angle, lunar eclipse, orbit precession, attitude constraints, and heat dissipation), and cargo handover is also carried out in this region; while passing quickly through the lunar night region (perilune), dependence on battery storage is reduced; at the same time, the 30 km (perilune) helps shorten the delivery distance and concentrate the energy supply to the area below, and also allows immediate regulation and compensation of spacecraft instability to prevent lunar-impact events. It should be noted that keeping the apolune always in the lunar day region requires the line of apsides to precess by about 360° per year following the solar direction (about 1°/day), which must be maintained by orbit design (using the Moon's J_2 and third-body perturbations) or by additional ΔV; the maintenance cost of a 30 km perilune under mascon perturbations is high (Table 4: 35–65 m/s·a for a 30 km orbit), and elliptical orbits must be checked orbit by orbit. The net benefit of this configuration remains to be verified numerically.

4.3 Orbital Energy Management: Ejection-Induced Orbit Change, Prograde/Retrograde Evolution, and Formation Scheduling

Suppose the platform ejects cargo prograde (in the same direction as the Moon's rotation); the platform gains a reverse impulse, its kinetic energy decreases, and its orbit lowers. The orbital evolutions caused by prograde and retrograde ejection are in opposite directions, and the effects of mascon perturbations on prograde and retrograde orbits differ (Appendix B), which allows flexible scheduling. Going further, cargo vessels of different masses/speeds can be arranged to enter port by "elastic coupling", so that the kinetic-energy difference between the two is gradually converted into stored electric energy through electromagnetic coupling during the adjustment (the principle is similar to momentum-exchange tethers/electromagnetic damping [47]), thereby achieving smooth regulation of the platform-port orbit at the energy level; this momentum–energy exchange mechanism is still at the concept stage and needs

to be verified through orbital dynamics propagation, ejection-mechanism tests, and cargo-flow optimization. The prograde/retrograde alternation of "orbit raising – orbit lowering" is just like the change of the water-depth line (draft line) caused by rising and falling tides, and can give rise to a corresponding theory of space engineering. Consistent with Sections 3.3 and 4.2.1, delivery to the lunar surface can only be made by backward ejection, and the stability and energy budget of this back-and-forth regulation must be verified by orbital dynamics simulation.

At the formation level, multiple platform ports operate interwoven in frozen orbits of different inclinations and non-co-rotating directions, forming an ellipsoidal lunar orbit network (Fig. 14) in which they back each other up and relay each other; unloaded platforms can carry high-specific-impulse electric propulsion or solar sails [7] to maintain their orbits, while loaded platforms maintain theirs by exchanging ejected propellant (cargo), with the goal of reducing dependence on propellant resupply from Earth; in real missions, independent propellant budgets must still be reserved for fault recovery, attitude control, and long-term orbit maintenance. Distributed platforms in different lunar orbits, like the multi-level steps of a stairway in lunar space, perform different functions between Earth and the Moon.

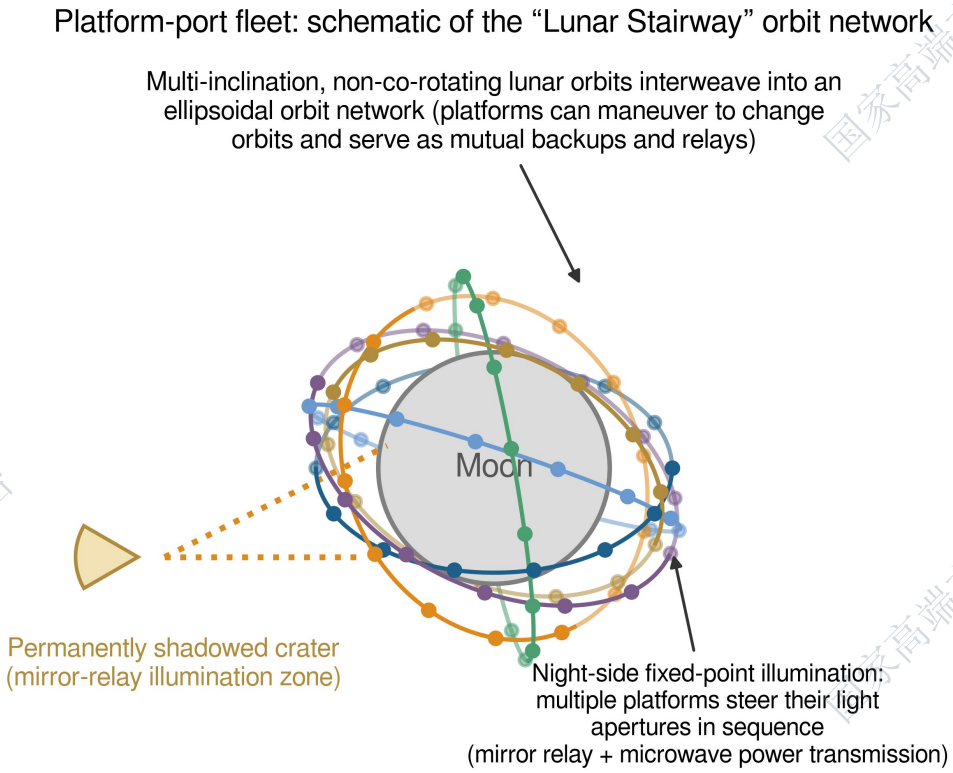


Fig. 14. Schematic of the multi-platform lunar orbit network and energy illumination

4.4 Energy, Illumination, and Microwave Power Transmission

The lunar night lasts as long as 14.6 Earth days and is the greatest weakness of the energy structure of the lunar surface paradigm; an orbital platform, although it experiences periodic lunar eclipses, is vastly different from the lunar surface in period, and long-term energy constraints can be reduced through orbit selection, power-system redundancy, and energy-storage management: a low-orbit platform is in

sunlight most of the time, and a high-orbit platform (for example, one that flattens the eccentricity in the lunar day region) can further extend the sunlit window. The platform can perform three functions: ① relaying sunlight from high-orbit regions by mirrors to the lunar night side and to permanently frozen craters; continuous illumination of PSR floors can vaporize water ice and make possible "a thermostatically controlled town under a transparent dome" on the crater floor [28, 29]; ② multiple platform ports can carry and concentrate reflecting-mirror groups to form a tandem constellation. When a platform enters the lunar night region, an intelligent seamless beam-pointing system directs a spotlight or microwave energy beam at a specific working area on the lunar surface, such as a lunar mining site or a base receiving ejected cargo (keeping the working temperatures of the capture-station energy storage, cryogenic magnets, and lubricated parts). Intelligent steering for fixed-point illumination and sequential navigation achieves stable illumination of fixed regions in the night region and provides relay-network coverage over a wide lunar area. Physical limits of mirror relay: the angular diameter of the solar disk is about 9.3 mrad, so the diameter of the light spot reflected by a flat mirror is no less than 9.3 mrad × distance, that is, about 0.93 km at 100 km (about 2.8 km at 300 km and about 9.3 km at 1,000 km); if the mirror diameter is smaller than the spot, the irradiance on the lunar surface falls as (mirror diameter/spot diameter)², for example, a 100 m aggregate mirror at 100 km can provide only about 1% of the solar constant (about 16 W/m²), and reaching the illumination requirement would require a mirror diameter close to 300 m. In addition, the visible time of a 100 km orbit platform for a given location (elevation > 30°) is only about 3 min per revolution, so continuous illumination would require about 36 platforms in relay. Mirror-relay illumination is therefore applicable only to small-area, low-power-density, or intermittent needs, and this "stable illumination" remains a concept; ③ energy-supply installations provide "cover-beam energy" from above for work on the lunar surface, transmitting power to the lunar surface by wireless power transfer (WPT), where electromagnetic energy-conversion devices convert it into electric power. Since Glaser [33] proposed the space solar power station, Caltech's MAPLE completed the first in-orbit space microwave power transfer demonstration in 2023 [34], providing the first flight data for its engineering (but the transmitted power and distance of that demonstration differ by several orders of magnitude from the hundred-kilowatt to megawatt level and hundred-kilometer level needed here; estimated at 5.8 GHz, a transmitting aperture of 100 m, and a distance of 100 km, the main-lobe spot diameter is about 126 m ($2.44\lambda R/D$), likewise limited by the visible time of about 3 min per revolution, so multiple platforms must relay). The cover-beam method is flexible for supplying energy to the Moon, and its orbit inclination and altitude can be scheduled dynamically, so that it is not restricted to particular regions. If throughput and power demand rise further, small nuclear power stations may also be considered: the United States, China, and Russia have all proposed building small nuclear facilities on the lunar surface by 2036 at the latest, but moonquakes and meteoroids will inevitably increase the risk of nuclear leakage, and protective measures will also add cost. If high-power small modular reactors (SMRs) are installed on Lunar Orbital Port platforms as mobile "nuclear-powered ports", the risk of ground leakage caused by moonquakes and meteoroids can be avoided (the UN Principles Relevant to the Use of Nuclear Power Sources in Outer Space must also be followed [52]), and surplus energy can also be transmitted by cover beam to the lunar surface or relayed to other platforms.

4.5 In-Orbit Manufacturing and Zero-Gravity Factories

A platform port can dock small zero-gravity factories: with no moonquake disturbance, no dust, and the ability to maneuver to avoid meteoroids, it is especially suited to precision smelting and manufacturing

(such as alloys, optical fibers, and semiconductor crystals). Under microgravity, the assembly of large-scale structures (such as trusses, antennas, and solar sails) requires no heavy ground lifting equipment; the factory's products can either be used in orbit or be shipped to the lunar surface or Earth with cargo vessels. The zero-gravity environment also offers unique experimental value for pharmacology and materials science. Whereas for a manufacturing base placed in a lunar surface factory, apart from a few locations (such as permanently sunlit zones and lava tubes) the Moon is an extremely hot environment, and temperature maintenance, lunar dust interference, moonquakes, meteoroids, and radiation are all weaknesses; in terms of protection and operating expenses, early lunar surface conditions are not the optimal choice.

4.6 Computing-Power Heat Dissipation and "Thermal-Mass Delivery"

Heat dissipation of space computing platforms (data centers, token factories, deep reasoning) is currently a hot topic. In vacuum, heat is dissipated mainly by radiation: by the Stefan–Boltzmann law, the radiated power of a 300 K blackbody surface is about 459 W/m², so a platform of the hundred-kilowatt class needs a radiator of the order of 220 m², which is mature engineering. This paper further proposes "thermal-mass delivery" as an auxiliary heat-dissipation concept: a dedicated platform module dissipates heat through its bulkhead and is loaded with liquid-phase/phase-change "thermal articles" of high heat capacity (latent heat of phase change about 200–400 kJ/kg), and the "ejection–capture" channel is used to deliver heat with the articles to the lunar night side; the articles re-solidify on the lunar surface at night and are launched back to the platform, circulating to cool the computing devices. But calculation shows that if a continuous thermal load of 100 kW relied entirely on phase-change material to carry it, about 1,440 kg/h would be needed (at 250 kJ/kg), which is a large quantity, so this method is suited only as a means of peak shaving for peak thermal loads, and radiators remain the main path; the idea of "using the Moon as a heat-dissipation sink" still has exploratory value; for example, because temperature differences on the lunar surface are extreme, existing research directions pour phase-change material into sintered regolith bricks to make intelligent building blocks that both bear loads and store and release heat, so the demand on the Moon for phase-change materials as a building material is predicted to be very large and is a hard requirement. Phase-change cargo shipped from Earth can therefore be sent first to the computing module for heat storage and then ejected to the Moon to make regolith bricks, satisfying the heat-dissipation needs of space computing in a continuous cargo-transfer mode.

4.7 Upward Transport of Lunar Surface Materials: Electromagnetic Ejector

Upward transport of materials from the lunar surface to lunar orbit can use electromagnetic ejection (a mass driver) [35, 36]: accelerating the payload to about 1.7 km/s is enough to enter LLO, with a kinetic energy of about 406 kWh/t; this electromagnetic ejection installation, operated in reverse (linear-motor generator braking/eddy-current braking), can be converted into the long-slope electromagnetic deceleration track described in Section 4.2.2, achieving an energy closed loop of "upward acceleration – downward recovery" [63, 65, 67]. The electromagnetic drive efficiency can exceed 90% [35], far surpassing the energy consumption of chemical propulsion; the low gravity and vacuum of the Moon make it an ideal electromagnetic launch site. Recent research shows that lunar gravity anomalies can also be exploited to fine-tune the ejection trajectory [36]. On the lunar-orbit side, the platform port or a dedicated catcher performs rendezvous and capture, completing the "lunar surface – lunar orbit" closed loop. Raw materials mined on the lunar surface and manufactured products can thus be transported

upward to orbit at low cost for processing, further weakening the necessity of "having to be stationed on the lunar surface". Note: cargo launched horizontally from the lunar surface at about 1.70 km/s has its perilune at the launch point (the surface), and must be captured by the platform at the 100 km apolune (where the speed is about 1.610 km/s, 23 m/s slower than the platform) or be circularized at apolune by the cargo's own small thrust; otherwise it will strike the lunar surface again; the electromagnetic acceleration section needs about 1.5 km at 100 g and about 14.7 km at 10 g. This upward logistics and the downward logistics of Section 4.2 form a momentum closed loop in Section 3.3. The same long slope can both launch in the forward direction and capture in the reverse direction, the two being time-multiplexed: the electric energy recovered by capturing 1 t of cargo can meet about 70% of the electricity consumed by an upward launch of the same mass, and the spindle, after being loaded at the entrance platform, can be reused for upward launch (see Section 4.2.3).

4.8 On In-Situ Resource Utilization

In-situ resource utilization (ISRU) is often taken as the core argument for lunar surface bases: using regolith to produce oxygen, extracting water ice, and 3D-printing building materials. But the maturation of ISRU requires a great deal of preliminary verification and equipment deployment, and itself depends on reliable lunar landing and long-term residence capability. Before ISRU technology matures, a lunar-orbit platform offers an agile scheme that can operate without ISRU: materials are shipped from Earth and relayed in orbit, in-situ resources are ejected to the lunar port, and finished products are stored or delivered back to the Moon at low cost.

ISRU and the lunar-orbit scheme are not in opposition. With the support of a lunar-orbit platform, the verification of ISRU can be carried out more calmly: small test equipment is lowered and delivered via the orbital platform, data are relayed back to Earth through the lunar-orbit platform, the cost of failure is far lower than that of a crewed lunar surface mission, and the lunar-orbit platform also provides more habitats for personnel.

4.9 Earth–Moon Materials Cycle and "Hull Orbitalization"

The lunar crust lacks siderophile elements, and such metals, which are abundant on Earth, are instead very scarce on the Moon. The nickel content of lunar basalts is usually below 100 ppm, and siderophile elements (Ni, Ir, Au, Re, Os, and so on) in lunar rocks are depleted overall by about a factor of 20–50 relative to Earth's mantle [26]; elemental metallic iron is less than 1 wt% in lunar rocks and is mostly dispersed as submicroscopic grains in the regolith (about 0.5–1.5 wt%), coming mainly from meteoritic input [26]. Reducing metals from silicates/oxides requires complete sets of smelting facilities and large amounts of energy, which is almost infeasible in the early stage. By comparison, finished steel is extremely plentiful on Earth: global crude steel output in 2024 was about 1.88 billion tonnes [42], annual nickel output is also in the millions of tonnes, and steel is one of the cheapest engineering metals on Earth. For lunar development, smelted steel is precisely a scarce asset to which the saying "the rarer, the more precious" applies.

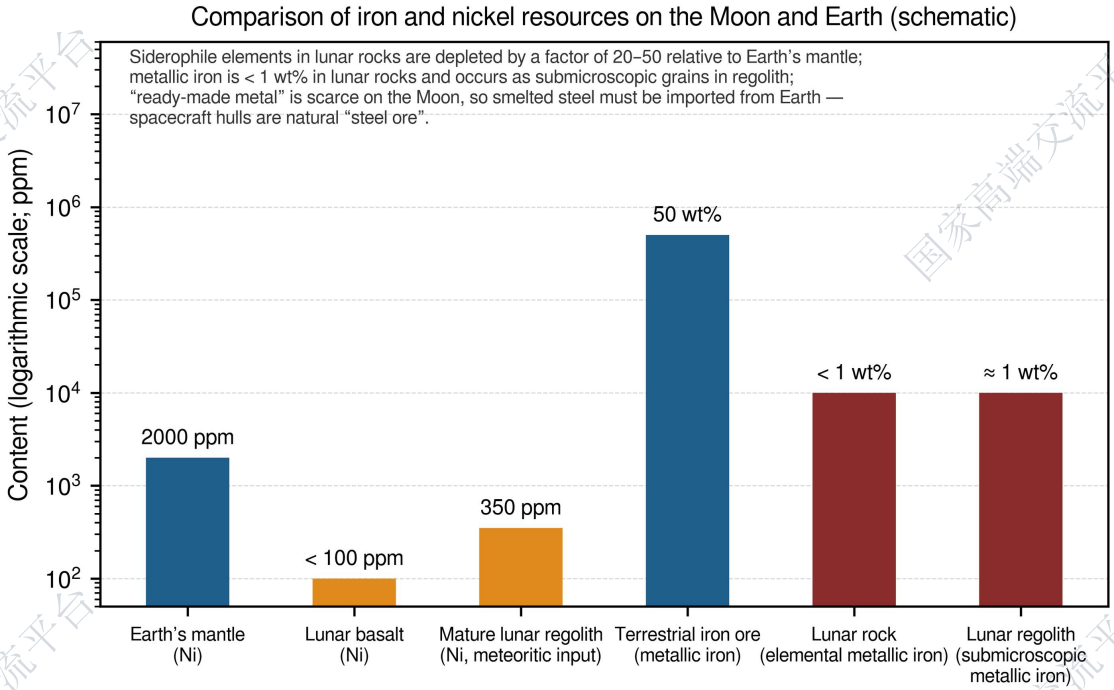


Fig. 15. Comparison of iron and nickel resources of the Moon and Earth (schematic; content orders of magnitude after the literature [26])

On this basis, this paper advocates "thinking one step further": the hulls of today's mainstream launch vehicles and spacecraft are mostly made of stainless steel, which is heavy, cheap, and durable, and is precisely the cheapest "steel ingot" that humans can transport to the Moon. After a hull completes its lunar mission, rather than returning it to Earth for reuse, it is better to leave it in lunar orbit to become a "floating cabin in lunar space" and a metal reserve (a logical extension of Fig. 15). Such hulls can serve as extension modules of a platform port, as temporary attached cabins, and even as carriers of small nuclear installations, and are also a raw-material depot for future smelting in lunar construction. Some cargo spacecraft can therefore be considered for design as one-way vehicles, with the residual bodies left in lunar orbit as platforms. When the scale of lunar logistics grows, dedicated "ingot ships", together with residual vessel hulls, will convert Earth's surplus production capacity into fixed assets on the Moon.

The economic logic of this strategy is intuitive: the cost of returning a hull (propellant, landing system, refurbishment) is far higher than the cost of maintaining and using the hull in lunar orbit, while the long-term value of the hull material in lunar orbit (as construction raw material or shielding) is far higher than its value as scrap metal on the ground, and there is no reentry pollution.

5 Orbital Habitability and Outlook for Long-Term Residence

Large platform ports, as "flying floating islands", may in the future take on many functions such as long-term residence, scientific research, manufacturing, and observation, creating gardens, art centers, unmanned factories, cinemas, and viewing domes inside sky cities; a metal shell covered with polyethylene/water/regolith blocks can block cosmic radiation. People will be able to gaze at the lunar surface at close range from the lunar skyport, and may also make brief "leisure trips" to the lunar surface under protection, and a future cluster of lunar-space cities may even develop. The long-term life of future lunar ports calls to mind the "Tanka people" (Dan people) of China's South China Sea, who have lived on boats for generations. If the habitability of lunar space remains consistently higher than that of the

Moon, we can likewise imagine a population living and evolving steadily for generations on "ship-islands" circling a planet, using the planet's gravitation for low-power maintenance, traveling from time to time between neighboring planets, and occasionally setting out for more distant places. Orbital life is not "settling for second best" but may be a civilizational form chosen by design: the space springboard envisioned by humankind is not built on the Moon but in lunar space, and it is also the starting point of Earth's "generational voyage" through space (the greatest advantage of the lunar-space launch port is that it spares the rocket the most energy-consuming initial acceleration stage, equivalent to saving an entire stage of rocket structure; on Earth, the first stage of a rocket accounts for about 45% of the hardware cost of the whole rocket and consumes more than 80% of the propellant of the whole rocket). If space agencies can adopt this proposal, adjusting space strategy can reduce the enormous cost of changing course.

This paper poses a systematic challenge to the lunar development paradigm centered on lunar surface stationing, and demonstrates the multidimensional advantages of the near-lunar-orbit platform architecture in the early stage of development. A further conclusion: orbital stationing is not limited to the Moon; human exploration of a planet should proceed from observation of its surroundings to familiarity, and entry should follow only once there is real confidence, as is true for any unfamiliar celestial body.

6 Projected Technology Timeline

Table 12. Phased timeline of the "Lunar Orbital Port"

Phase	Time window	Main content	Key milestones	Main risks and countermeasures
1. Pilot verification	T0 to T0+5 years (T0 is the project-approval year)	Small verification ejection capsule; scaled long-slope electromagnetic capture test (sub-km class); blind-ejection calibration and capture impact-point model, mid-course correction and terminal guidance verification; small-mass ballistic delivery; scaled electromagnetic deceleration-track test; electric-propulsion platform-port prototype	First successful long-slope electromagnetic deceleration capture with electric energy recovered; perilune altitude control accuracy reaching the ±100 m order (terminal guidance required); scaled deceleration track completing dissipation verification	Guidance accuracy and regenerative braking efficiency: verify first at small mass in scale and measure the recovery efficiency; reliability of the guide channel/levitation and impact-point deviation: control through redundant trial deliveries and iteration of the gravity field model
2. Platform Port No. 1	T0+5 to T0+10 years	Platform port in a 30–100 km near-lunar orbit; routine ballistic delivery; verification of lunar surface electromagnetic ejection; cargo-vessel cabin-attachment transfer	Platform port enters orbit and operates continuously for more than 2 years; annual throughput of the 1,000 t class; must pass the break-even review of Section 3.7 (threshold of cumulative delivered mass about 300 t–1,000 t)	Impact g-load constraints on payloads: formulate a cargo-container g-load specification; orbit maintenance depends on electric propulsion
3. Formation and energy network	T0+10 to T0+18 years	Multi-platform formation and orbit network; mirror-relay illumination; microwave power transmission; zero-gravity factory; feasibility study of the nuclear-powered port	Demonstrations of night-side fixed-point illumination and PSR water-ice mining; in-orbit factory in production	Power-transmission efficiency and nuclear approval: non-nuclear schemes first
4. Lunar surface outposts and closed loop	After T0+18 years	A small number of crewed lunar surface outposts; large-scale storage of residual vessel hulls in lunar orbit; closed Earth–Moon materials cycle	Lunar surface outposts achieve energy/water self-sufficiency; metal stored in lunar orbit reaches the 10,000 t level	Lunar-orbit debris management and long-term residence medicine: establish registration and traffic rules

Note: (1) The time windows are indicative planning and are adjusted with actual investment and technical verification, being revised on a rolling basis according to test data and mission conditions.
Note: (2) Deploying living and production clusters in lunar orbit greatly enlarges the range of human space activity, and this system of human cooperation relatively reduces the significance of symbolic lunar surface sovereignty activities represented by "flag planting".
Note: (3) A decision threshold is set at each phase: without passing the guidance-accuracy, regenerative-braking-efficiency, and break-even reviews of the previous phase, the next phase is not entered; time windows are expressed in relative years and do not constitute a schedule commitment.

7 Near-Term Verifiable Work

(1) In-orbit verification of the relative navigation and mid-course correction of a capsule (with the perilune set above the surface, not touching the Moon, and continuing its flight after passing); (2) ground-based scaled electromagnetic/eddy-current deceleration-track tests to obtain data on peak power and regeneration efficiency; (3) regenerative-braking tests of a linear synchronous motor at speeds of 0.1–1 km/s, to establish the braking force–speed–recovery efficiency relationship, and verification of levitation and guidance on a high-speed sled track; (4) accumulation of in-orbit data on long-term maintenance of frozen orbits; (5) full-process tests of the long-slope entrance guide funnel and spindle at low speed (≤ 50 m/s) covering levitation, track entry, and roll-back, together with centrifuge and shock qualification of a 1 t/30 g-class reinforced cargo bay.

References

[1] Muller P M, Sjogren W L. Mascons: lunar mass concentrations. *Science*, 1968, 161(3842): 680–684.

[2] Zuber M T, Smith D E, Watkins M M, et al. Gravity field of the Moon from the Gravity Recovery and Interior Laboratory (GRAIL) mission. *Science*, 2013, 339(6120): 668–671.

[3] Lemoine F G, Goossens S, Sabaka T J, et al. GRGM900C: a degree 900 lunar gravity model from GRAIL primary and extended mission data. *Geophysical Research Letters*, 2014, 41(10): 3382–3389.

[4] Elipe A, Lara M. Frozen orbits about the Moon. *Journal of Guidance, Control, and Dynamics*, 2003, 26(2): 238–243.

[5] Mazarico E, Neumann G A, Barker M K, et al. Orbit determination of the Lunar Reconnaissance Orbiter: status after seven years. *Planetary and Space Science*, 2018, 162: 2–19.

[6] Song Y-J, Lee D, Kim Y-R, et al. Analysis on delta-Vs to maintain extremely low altitude on the Moon and its application to CubeSat mission. *Journal of Astronomy and Space Sciences*, 2019, 36(3): 213–223.

[7] Station-keeping approach for extremely low lunar orbits with solar sailing. arXiv:2606.05601, 2026.

[8] Wertz J R, Larson W J. *Space Mission Analysis and Design*. 3rd ed. El Segundo: Microcosm Press, 1999.

[9] Bate R R, Mueller D D, White J E. *Fundamentals of Astrodynamics*. New York: Dover Publications, 1971.

[10] Freeman R H. Soft landing on the Moon: the ups and downs of robotic lunar landers. *Space Operations Communicator*, 2025, Q2B.

[11] AP News. Here's a look at moon landing hits and misses. (2025-03-07). https://apnews.com/article/moon-landings-failures-successes-545ea2f3ffa5a15893054b6f43bdbb98.

[12] The Moon mission catalog. azmth.space. https://azmth.space/moon/missions.

[13] JAXA. Outcome for the Smart Lander for Investigating Moon (SLIM)'s Moon landing. (2024-01-25). https://global.jaxa.jp/press/2024/01/20240125-1_e.html.

[14] ispace. ispace releases technical cause analysis for HAKUTO-R Mission 2. (2025-06-24). https://www.ispace-inc.com/2025/06/24/ispace-releases-technical-cause-analysis-for-hakuto-r-mission-2/.

[15] NASA. NASA receives some data before Intuitive Machines ends lunar mission. (2025-03-07). https://www.nasa.gov/news-release/nasa-receives-some-data-before-intuitive-machines-ends-lunar-mission/.

[16] Nakamura Y, Latham G V, Dorman H J, et al. Apollo lunar seismic experiment—final summary. *Journal of Geophysical Research*, 1982, 87(S01): A677–A690.

[17] Nakamura Y. Seismic risk for the lunar base. In: Mendell W W, ed. *Lunar Bases and Space Activities of the 21st Century*. Houston: Lunar and Planetary Institute, 1985.

[18] Neal C. The importance of establishing a global lunar seismic network. LEAG 2005. https://www.lpi.usra.edu/meetings/leag2005/presentations/tues_am/06_neal.pdf.

[19] Grün E, Zook H A, Fechtig H, et al. Collisional balance of the meteoritic complex. *Icarus*, 1985, 62(2): 244–272.

[20] Kuchner M, et al. Meteoroids at the Moon: orbital properties, surface vaporization, and impact ejecta production. NASA NTRS 20210011054, 2021.

[21] Micrometeoroid impact rate analysis for an Artemis-era lunar base. arXiv:2511.04740, 2025.

[22] Zhang S, Wimmer-Schweingruber R F, Yu J, et al. First measurements of the radiation dose on the lunar surface. *Science Advances*, 2020, 6(39): eaaz1334.

[23] Matthiä D, Berger T. Radiation exposure and shielding effects on the lunar surface. *Space Weather*, 2024, 22(12): e2024SW004095.

[24] NASA. Lunar dust technical brief: OCHMO-TB-011 Rev C. 2023.

[25] Linnarsson D, Carpenter J, Dambis B, et al. Toxicity of lunar dust. *Planetary and Space Science*, 2012, 74(1): 57–71.

[26] Heiken G H, Vaniman D T, French B M, eds. *Lunar Sourcebook: A User's Guide to the Moon*. Cambridge: Cambridge University Press, 1991.

[27] Murphy D M, Abou-Ghanem M, et al. Metals from spacecraft reentry in stratospheric aerosol particles. *Proceedings of the National Academy of Sciences*, 2023, 120(43): e2313374120.

[28] Li S, Lucey P G, Milliken R E, et al. Direct evidence of surface exposed water ice in the lunar polar regions. *Proceedings of the National Academy of Sciences*, 2018, 115(36): 8907–8912.

[29] Colaprete A, Schultz P, Heldmann J, et al. Detection of water in the LCROSS ejecta plume. *Science*, 2010, 330(6003): 463–468.

[30] Woods A, Vogler A, Collins P. The lunar space elevator: a key technology for realising the Greater Earth Lunar Power Station (GE⊕-LPS). Astrostrom GmbH. https://astrostrom.ch/docs/JBIS-6-Lunar-Space-Elevator.pdf.

[31] Pearson J, Levin E M, Oldson J, et al. Lunar space elevators for cislunar transportation. NIAC Phase I Final Report, NASA, 2005.

[32] Penoyre Z, Sandford E. The Spaceline: a practical space elevator alternative achievable with current technology. arXiv:1908.09339, 2019.

[33] Glaser P E. Power from the sun: its future. *Science*, 1968, 162(3856): 857–861.

[34] Hajimiri A, et al. Wireless power transfer in space using flexible, lightweight, coherent arrays. arXiv:2401.15267, 2024.

[35] O'Neill G K. *The High Frontier: Human Colonies in Space*. New York: William Morrow, 1977.

[36] Launching mass from the Moon helped by lunar gravity anomalies. arXiv:2410.09616, 2024.

[37] Zhang L. Development and prospect of Chinese lunar relay communication satellite. *Space: Science & Technology*, 2021: 3471608.

[38] NASA. Artemis Accords. (2020). https://www.nasa.gov/artemis-accords/.

[39] CNSA, ROSCOSMOS. Joint statement regarding cooperation for the construction of the International Lunar Research Station. (2021). http://www.cnsa.gov.cn/english/n6465652/n6465653/c6811967/content.html.

[40] An imaging algorithm for a lunar orbit interferometer array. arXiv:1805.08259, 2018.

[41] NASA. Lunar Crater Radio Telescope (LCRT) on the far-side of the Moon: NIAC Phase 2 Report. NASA NTRS 20250001334, 2025.

[42] World Steel Association. December 2024 crude steel production and 2024 global crude steel production totals. (2025-01-24). https://worldsteel.org/media/press-releases/2025/december-2024-crude-steel-production-and-2024-global-totals/.

[43] NASA. Apollo 11 Flight Plan (Final). Houston: Manned Spacecraft Center, 1969.

[44] NASA. Apollo mission techniques: lunar orbit activities. NASA NTRS 20090015331, 2009.

[45] NASA. Apollo 11 Mission Report: SP-238. Houston: Manned Spacecraft Center, 1969.

[46] The Planetary Society. 2025 NASA Innovative Advanced Concepts symposium: part 1 — lunar glass and starshades (LUNGS). (2025). https://www.planetary.org/planetary-radio/2025-niac-symposium-part-1.

[47] Cosmo M L, Lorenzini E C. *Tethers in Space Handbook*. 3rd ed. Cambridge: Smithsonian Astrophysical Observatory, 1997.

[48] Whitley R, Martinez R. Options for staging orbits in cislunar space. In: *2016 IEEE Aerospace Conference*. Big Sky: IEEE, 2016.

[49] Zeitlin C, Hassler D M, Cucinotta F A, et al. Measurements of energetic particle radiation in transit to Mars on the Mars Science Laboratory. *Science*, 2013, 340(6136): 1080–1084.

[50] Simonsen L C, Nealy J E. Radiation protection for human missions to the Moon and Mars. NASA TP-3079, 1991.

[51] Gibson L J, Ashby M F. *Cellular Solids: Structure and Properties*. 2nd ed. Cambridge: Cambridge University Press, 1997.

[52] United Nations General Assembly. Principles Relevant to the Use of Nuclear Power Sources in Outer Space. Resolution 47/68, 1992.

[53] Inter-Agency Space Debris Coordination Committee. IADC Space Debris Mitigation Guidelines. IADC-02-01.

[54] United Nations. Treaty on Principles Governing the Activities of States in the Exploration and Use of Outer Space, including the Moon and Other Celestial Bodies. 1967.

[55] Arnold W H, Bowen S, Cohen S, et al. Mass drivers III: engineering. In: *Space Resources and Space Settlements*. NASA SP-428. Washington, DC: NASA, 1979: 119–157.

[56] Doyle M R, Samuel D J, Conway T, et al. Electromagnetic aircraft launch system—EMALS. *IEEE Transactions on Magnetics*, 1995, 31(1): 528–533.

[57] NAVAIR. Advanced Arresting Gear (AAG). https://www.navair.navy.mil/product/Advanced-Arresting-Gear-AAG.

[58] Reitz J R. Forces on moving magnets due to eddy currents. *Journal of Applied Physics*, 1970, 41(5): 2067–2071.

[59] Post R F, Ryutov D D. The Inductrack approach to magnetic levitation. *IEEE Transactions on Applied Superconductivity*, 2000, 10(1): 901–904.

[60] Boldea I, Nasar S A. *Linear Electric Actuators and Generators*. Cambridge: Cambridge University Press, 1997.

[61] Holloman AFB. Test track takes levitation to new speeds. https://www.holloman.af.mil/News/Display/Article/318531/test-track-takes-levitation-to-new-speeds/.

[62] Holloman High Speed Test Track. https://en.wikipedia.org/wiki/Holloman_High_Speed_Test_Track.

[63] Heppenheimer T A. A lunar mass transportation system. 1991. (NASA NTRS: 19910073677)

[64] General Atomics. EMALS & AAG: aircraft launch & recovery system. https://www.ga.com/defense/alre.

[65] Xiong J Y, Shen Z Y, Chi M R, et al. A review of high-speed maglev train technology. *Journal of Traffic and Transportation Engineering*, 2025, 25(2): 1–23 (in Chinese).

[66] Zeng F F, Chen J D, Wang X Y, et al. Braking system of maglev trains. *Electric Drive for Locomotives*, 2025 (in Chinese).

[67] Central Japan Railway Company. Regenerative braking of SCMAGLEV. https://scmaglev.jr-central-global.com/about/emergency/.

国家高端交流平台

Appendix A List of Symbols

Table A1. Principal symbols

Symbol	Meaning	Value/unit
R_m	Mean lunar radius	1,737.4 km
μ_m	Lunar gravitational constant	4,902.8 km³/s²
g_0	Standard gravitational acceleration of Earth	9.81 m/s²
g_m	Gravitational acceleration at the lunar surface	1.624 m/s²
ΔV	Velocity increment	km/s or m/s
I_{sp}	Specific impulse	s
m_0 / m_1	Initial / final mass	t
a	Orbital semi-major axis	km
T	Orbital period	h
v_{circ}	Circular orbit speed	km/s
r_{Hill}	Hill sphere radius of the Moon	≈ 6.15×10^4 km
L	Effective deceleration stroke of the long slope	km
n	Mean deceleration g-load (in units of g_0)	g
E	Impact kinetic energy	GJ
TNT equivalent	Energy conversion	kg
θ_e	Terminal slope of the long slope (vertical curve)	° (baseline 3°)
R_c	Radius of curvature of the vertical curve	km (baseline ≈ 115)
P	Regenerative braking power	MW
η	Overall energy recovery efficiency	0.786 (assumed)
m	Total mass of the payload capsule	1.2 t (cargo 1 t + spindle 0.2 t)

Appendix B Calculation Parameters and Assumptions

(1) Orbit calculation: circular orbit speed $v_{circ} = (\mu_m/r)^{1/2}$, period $T = 2\pi(a^3/\mu_m)^{1/2}$; R_m = 1737.4 km and μ_m = 4902.8 km³/s² are adopted as the unified parameters of the two-body approximation in this paper. Ballistic delivery model: the platform is in a 100 km circular orbit (v = 1.633 km/s); after ejection it enters a transfer ellipse with perilune r_p = 1,737.4 km and apolune r_a = 1,838.4 km, with ejection increment $\Delta V_{ej} = v_{circ} - v(r_a) = 1.633 - 1.610 \approx 0.023$ km/s; the touchdown speed is evaluated at perilune by the vis-viva equation, $v_p \approx 1.70$ km/s, with direction mainly horizontal.

(2) Rocket equation: $m_{prop}/m_0 = 1 - \exp(-\Delta V/(I_{sp}\cdot g_0))$. For chemical propulsion I_{sp} is taken as 300 s (in the Table 4 comparison, 300 s for the ISS and 320 s for Earth–Moon transfer); for electric propulsion I_{sp} is taken as 1,600 s (typical value for a Hall thruster); for cold gas I_{sp} is taken as 70 s. The "chemical propellant/electric-propulsion propellant" columns in Table 4 are converted at the midpoint of the corresponding ΔV.

(3) Deceleration model: mean g-load $n = v^2/(2L\cdot g_0)$, taking v = 1,700 m/s and neglecting the vertical component (grazing entry) and the peak effect of the regenerative braking force limit/jerk ramp (about +9%, Table 9); this formula is used only for a first-order scale estimate of the mean deceleration and does not represent the true impact peak, which must be determined by scaled electromagnetic braking tests or an explicit dynamic model.

(4) Radiation dose: the lunar surface background cites the Chang'E-4 LND measurements [22]; the SPE

cites the NASA 1988 estimate and the latest shielding modeling results [23]; "about 1.1–1.3 mSv/d in a lunar-orbit cabin after 20 g/cm² shielding" is estimated in this paper by multiplying the MSL RAD cruise-phase measured dose-equivalent rate (about 1.8 mSv/d) [49] by (1 − blocking fraction by the Moon), where the blocking fraction is $(1 - \cos \rho)/2$ with $\rho = \arcsin[R_m/(R_m + h)]$ (about 41%, 34%, and 28% for 30, 100, and 200 km, respectively), to be corrected by in-mission measurements.

(5) Orbit maintenance: the ΔV intervals are synthesized from the literature [6–8] and the LRO measurements [5]; the ISS reboost $\Delta V \approx 57$ m/s and propellant of about 7.5 t/a (total mass about 420 t) are taken from public flight data [8].

(6) Energy and mass accounting: the electromagnetic ejection kinetic energy is calculated as $0.5mv^2$ (v = 1.71 km/s, corresponding to the LLO transfer entry), about 406 kWh/t; conceptual contents such as long-slope regenerative braking energy recovery and thermal-mass delivery are all explicitly labeled "concept/estimate" and do not constitute an engineering commitment.

(7) Eclipse fraction: for a circular orbit ($\beta = 0$) the fraction of the orbital period spent in lunar eclipse is ρ/π, with ρ as above (about 44%, 39%, 35%, and 22% for 30, 100, 200, and 1,000 km, respectively).

(8) Perilune sensitivity: from conservation of angular momentum and the vis-viva equation, $h = r_a v_a$, $p = h^2/\mu$, $e = 1 - p/r_a$, $r_p = p/(1 + e)$; taking r_a = 1,837.4 km and $v_a = v_c - \Delta V_{ej}$, at the nominal ΔV_{ej} = 23 m/s $r_p \approx R_m$, and in its vicinity $dr_p/dv_a \approx 4.2$ km/(m/s). The along-track deviation (half a revolution of flight after ejection) is about 11 km/(m/s). The incidence angle is obtained from $\cos \gamma = h/(R_m \cdot v)$; at ΔV_{ej} = 24 m/s the perilune is about 4.2 km below the surface, with $\gamma \approx 0.65°$.

(9) Deceleration and energy absorption: stroke $L = v^2/(2n \cdot g_0)$; dissipated energy $E = \frac{1}{2}mv^2$ (v = 1.70 km/s; for 1 t, 1.445 GJ ≈ 401 kWh); consumable absorber mass $m_{abs} = E/\mathrm{SEA}$, with the specific energy absorption SEA taken as 10–30 kJ/kg (assumption); mean power $P = E/(2L/v)$.

(10) Recoil and propellant: $\Delta V_{plat} = M_p \cdot V_{rel}/(M_{plat} - M_p)$, V_{rel} = 23 m/s; the electric-propulsion propellant required for compensation is $m_{prop} \approx M_p \cdot V_{rel}/(I_{sp} \cdot g_0)$, about 1.2 kg/t at I_{sp} = 2,000 s.

(11) Break-even: $N^* = (M_{plat} + c_L \cdot M_{inf})/(c_L - c_B)$, c_L = 2.86, c_B = 1.2, with M_{plat} and M_{inf} taken as the illustrative values of Table 6; the LEO-to-LLO mass conversion is $m_{LEO}/m_{LLO} = \exp[4.0/(I_{sp} \cdot g_0)]$, about 2.5 and 3.1 for I_{sp} = 450 s and 360 s, respectively.

(12) Optics and microwaves: the diameter of the mirror-reflected spot ≥ 9.3 mrad × distance; the microwave main-lobe spot diameter ≈ $2.44\lambda R/D$ (f = 5.8 GHz, $\lambda \approx 5.2$ cm, D = 100 m, R = 100 km, about 126 m); the visible time is obtained from the central angle $\lambda = \arccos[R_m \cdot \cos(\mathrm{el})/(R_m + h)] - \mathrm{el}$ (el = 30°), about 3 min per revolution.

(13) Baseline example of long-slope capture: m = 1,200 kg, v_0 = 1,700 m/s, limit $a_{max} = 30\ g_0$, jerk $j = 60\ g_0$/s, braking to v_{stop} = 10 m/s; explicit integration of $dv/dt = -a(t)$ with a time step of 1 ms, with $a(t)$ following a "ramp up – plateau – ramp down" law, the ramp-down beginning when $v - a^2/(2j) = v_{stop}$; $F = m \cdot a$, $P = F \cdot v$, $E = \int P\, dt$; in the power-limited case $a = \min(a_{max}, P_{cap}/(m \cdot v))$, P_{cap} = 300 MW.

(14) Vertical curve and roll-back: $h(x) = x^2/(2R_c)$, $R_c = L/\theta_e$, L = 6 km, θ_e = 3°; roll-back acceleration $g_m \cdot (x/R_c)$, speed limit v_{cap}, with the final segment decelerated by regenerative braking at 0.3 m/s² to not more than 0.5 m/s.

(15) Potential-energy fraction: $\eta_{PE} = 2g_m \cdot L \cdot \sin\theta/v_0^2$; gravity stopping distance $s = v^2/(2g_m \cdot \sin\theta)$; the rise required for absorption entirely by potential energy is $H = v_0^2/(2g_m) \approx 890$ km.

(16) Energy-efficiency chain: $\eta = \eta_1 \cdot \eta_2 \cdot \eta_3 = 0.90 \times 0.97 \times 0.90 \approx 0.786$ (author's assumption); returnable electric energy = $\eta \cdot v_0^2/2$; electricity consumption for upward launch 406 kWh/t ÷ 0.90 ≈ 451 kWh/t (see Section 4.7).

(17) Eddy-current braking: $F(v) = 2F_{pk}/(v/v_c + v_c/v)$ (normalized form of the Reitz type), and for $v \gg v_c$, $F \approx 2F_{pk} \cdot v_c/v$, with power upper limit $2F_{pk} \cdot v_c$; skin depth $\delta = (\pi \cdot f \cdot \mu_0 \cdot \sigma)^{-1/2}$, $\sigma_{Al} = 3.5 \times 10^7$ S/m, $f = v/(2\tau)$, $\tau = 5$ m; magnetic pressure $B^2/(2\mu_0)$, about 0.4 MPa at $B = 1$ T.

(18) Approach corridor and funnel: $e = (r_a - r_p)/(r_a + r_p)$, $p = a(1 - e^2)$, $r(\Delta) = p/(1 + e \cdot \cos \Delta)$, $\Delta = d/R_m$, height = $r - R_m$ (r_a = 1,837.4 km, $r_p = R_m$); funnel wall-contact lateral speed $v_{lat} = v_0 \cdot w/L_f$, $w = 2$ m, L_f = 0.4 km; the ΔV required for go-around lift is $\approx 2\Delta h/t$ ($t = 30$ s; about 1.3 m/s at $\Delta h = 20$ m).